Since January 2020 Elsevier has created a COVID-19 resource centre with free information in English and Mandarin on the novel coronavirus COVID-19. The COVID-19 resource centre is hosted on Elsevier Connect, the company's public news and information website.

Applied Mathematical Modelling 97 (2021) 281–307

Contents lists available at ScienceDirect

Applied Mathematical Modelling

journal homepage: www.elsevier.com/locate/apm

Review of fractional epidemic models

Yuli Chen [a], Fawang Liu [b,c,*], Qiang Yu [b], Tianzeng Li [d]

[a] Fuzhou University Zhicheng College, Fujian 350001, China
[b] School of Mathematical Sciences, Queensland University of Technology, GPO Box 2434, Brisbane, QLD 4001, Australia
[c] College of Mathematics and Computer Science, Fuzhou University, Fujian 350116, China
[d] School of Mathematics and Statistics, Sichuan University of Science and Engineering, Zigong 643000, China

ARTICLE INFO

Article history:
Received 26 January 2021
Revised 4 March 2021
Accepted 23 March 2021
Available online 20 April 2021

Classification:
26A33
97M60
37M05
37N30

Keywords:
Epidemic models
Fractional order differential equations
Multi-term epidemic models
Parameter estimation
Implicit numerical method
Hybrid simplex search and particle swarm optimisation

ABSTRACT

The global impact of corona virus (COVID-19) has been profound, and the public health threat it represents is the most serious seen in a respiratory virus since the 1918 influenza A(H1N1) pandemic. In this paper, we have focused on reviewing the results of epidemiological modelling especially the fractional epidemic model and summarized different types of fractional epidemic models including fractional Susceptible-Infective-Recovered (SIR), Susceptible-Exposed-Infective-Recovered (SEIR), Susceptible-Exposed-Infective-Asymptomatic-Recovered (SEIAR) models and so on. Furthermore, we propose a general fractional SEIAR model in the case of single-term and multi-term fractional differential equations. A feasible and reliable parameter estimation method based on modified hybrid Nelder-Mead simplex search and particle swarm optimisation is also presented to fit the real data using fractional SEIAR model. The effective methods to solve the fractional epidemic models we introduced construct a simple and effective analytical technique that can be easily extended and applied to other fractional models, and can help guide the concerned bodies in preventing or controlling, even predicting the infectious disease outbreaks.

1. Introduction

Infectious diseases are generally considered as the enemy of human health in history and have continued to be the major causes of suffering and mortality in developing countries. It is well known that the spread of a communicable disease involves disease-related factors such as infectious agent, made of transmission, incubation period, infectious periods, susceptibility and resistance. Moreover, infectious disease agents adapt and evolve, so that new infectious diseases have emerged and some existing diseases have reemerged. Many identified diseases include Lyme disease (1975), Legionnaire's disease (1976), toxic-shock syndrome (1978), hepatitis C (1989), hepatitis E (1990), and hantavirus(1993). The human immunodeficiency virus (HIV), which is the etiological agent for acquired immunodeficiency syndrome (AIDS), emerged in 1981 and has become an important sexually transmitted disease throughout the world. Antibiotic-resistant strains of tuberculosis, pneumonia, and gonorrhea have evolved. Malaria, dengue, and yellow fever have reemerged and are spreading into new regions as climate changes occur. Diseases such as plague, cholera, and hemorrhagic fevers (Bolivian, Ebola, Lassa, Marburg, etc.) continue to erupt occasionally [1]. Since December 2019, an increasing number of cases of novel coronavirus (COVID-19) infected pneumonia (NCIP) have been identified in Wuhan, a large city of 11 million people in central China on 31 December

* Corresponding author.
E-mail address: f.liu@qut.edu.au (F. Liu).

https://doi.org/10.1016/j.apm.2021.03.044
0307-904X/

2019. The COVID-19 pandemic is now a major global health threat [2]. It is clear that human or animal invasions of new ecosystems, global warming, environmental degradation, increased international travel, and changes in economic patterns will continue to provide opportunities for new and existing infectious diseases [3]. The emerging and reemerging diseases have led to a revived interest in infectious diseases.

During the past 70 years, the study of infectious disease dynamics has matured into a rich interdisciplinary field at the intersection of mathematics, epidemiology, computational physics, ecology, evolutionary biology, immunology, sociology, and public health. Epidemiology is the branch of science which essentially deals with the mathematical modeling of spread of diseases, and mathematical modeling in epidemiology is concerned with describing the spread of disease and its effect on people [1]. This itself encompasses a range of disciplines, from biology, mathematics, and engineering to sociology and philosophy, all of which are utilized to a better understanding and predicting of the spread of infection [4–7].

One of the early triumphs of mathematical epidemiology was a formulation of a model in [8] to predict the behavior of a disease. In order to control the spread of infectious diseases, researchers have built a great deal of mathematical models to study the dynamical behavior of infectious diseases. Communicable disease models describing a directly transmitted vital or bacterial agent in a closed population. The formulation of a model is a process which includes statement of the relevant assumptions, relationship among variables, and parameters and relations governing their behaviors. Of course, the choice of these factors is critical to the model and depends largely on the particular disease to be modeled and the intended purpose of that model [6]. Mathematical models and computer simulations are useful experimental tools for building and testing theories, assessing quantitative conjectures, answering specific questions, determining sensitivities to changes in parameter values, and estimating key parameters from data [9–11]. The practical challenges range from establishing appropriate data collection to managing increasingly large volumes of information. The theoretical challenges require fundamental study of many-layered, non linear systems in which infections evolve and spread, and where key events can be governed by unpredictable pathogen biology or human behavior. Understanding the transmission characteristics of infectious diseases in communities, regions, and countries can lead to better approaches to decreasing the transmission of these diseases. Coupled to continuous dialogue between decision makers and the multidisciplinary infectious disease community, and by drawing on new data streams, mathematical models can lay bare mechanisms of transmission and indicate new approaches to prevention and control that help to shape national and international public health policy. By fitting these models with epidemiological data proper interpretation can be made through the estimated parameters. The numerical solutions for these models will be visualized via a graphical user interface which will allow users to tune the parameters to reveal important characteristics about the models and infectious diseases. As such, epidemiology modeling can contribute to the design and analysis of epidemiological surveys, suggest crucial data that should be collected, identify trends, make general forecasts, and estimate the uncertainty in forecasts [5].

Although a model for smallpox was formulated and solved by Daniel Bernoulli in 1760 in order to evaluate the effectiveness of variolation of healthy people with the smallpox virus, deterministic epidemiology modeling seems to have started in the 20th century [1]. In 1906 Hamer formulated and analyzed a discrete time model in his attempt to understand the recurrence of measles epidemics. His model may have been the first to assume that the incidence (number of new cases per unit time) depends on the product of the densities of the susceptibles and infectives. Ross was interested in the incidence and control of malaria, so he developed differential equation models for malaria as a host-vector disease in 1911. Other deterministic epidemiology models were then developed in papers by Ross, Ross and Hudson, Martini, and Lotka. Starting in 1926 Kermack and McKendrick published papers on epidemic models and obtained the epidemic threshold result that the density of susceptibles must exceed a critical value in order for an epidemic outbreak to occur. Mathematical epidemiology seems to have grown exponentially starting in the middle of the 20th century (the first edition in 1957 of Bailey's book is an important landmark), so that a tremendous variety of models have now been formulated, mathematically analyzed, and applied to infectious diseases. Reviews of the literature show the rapid growth of epidemiology modeling. The recent models have involved aspects such as passive immunity, gradual loss of vaccine and disease-acquired immunity, stages of infection, vertical transmission, disease vectors, macroparasitic loads, age structure, social and sexual mixing groups, spatial spread, vaccination, quarantine, and chemotherapy. Special models have been formulated for diseases such as measles, rubella, chickenpox, whooping cough, diphtheria, smallpox, malaria, onchocerciasis, filariasis, rabies, gonorrhea, herpes, syphilis, and HIV/AIDS. The breadth of the subject is shown in the books on epidemiology modeling [12,13].

The important mathematical model describing the evolution infectious diseases is called compartmental model which was originally established by Kermack and Mckendrick (1927) to study the spread of the infectious diseases [8]. In the compartmental system, the population is divided into three separate compartments, these compartments are defined with respect to disease status. Namely, the susceptible compartment S, the infected compartment I, and the removed compartment R. In the system, the susceptible person get infected and becomes an infected person making contact with an infected person, and the infected person can be recovered taking treatments, the individuals who reach this class have permanent immunity for the relevant disease. This type of model is called the SIR (susceptible-infected-removed) model whose variants are widely being studied and applied in studying specific disease such as dengue and leptospirosis epidemics.

Based on the Kermack-McKendrick model, various epidemic models have been developed in recent decades. The choice of which compartments to include in a model depends on the characteristics of the particular disease being modeled and the purpose of the model [1]. The passively immune class M and the latent period class E are often omitted, because they are not crucial for the susceptible-infective interaction. Acronyms for epidemiology models are often based on the flow patterns between the compartments such as MSEIR, MSEIRS, SEIR, SEIRS, SEIAR, SIR, SIRC, SIRS, SEI, SEIS, SI, SIS, SVIR, and

SVEIR (where S, V, I and R denote the populations of susceptible, vaccinated, infectious and recovered individuals). Such as SIS models in which system there exists a high possibility of recovered individuals to be re-injected. Depending on the actual disease, more or less of these classes may be used. For example, some disease models only include the S and I classes, while others may have a forth class which represents a state in which a disease is latent(SEIR models) or has a cross-immune state(SIRC models) such as Salmonella Bacterial infection. Diseases like Gonorrhea, Chagas and Rocky Mountain Spotted fevers are modeled using SIS models because people become susceptible as soon as the recover from infection. For disease like AIDS, influenza A(H1N1), measles, SEIR model is more appropriate as there is a latent period, when the virus is present in the host but has still not infected the host. And it is not suitable for modeling endemic diseases as it cannot display endemic behavior. It is more appropriate to propose multigroup epidemic models to describe the transmission dynamics of many infectious diseases in heterogeneous host populations, such as dengue fever, leptospirosis; some disease process includes the quarantined state such as measle, mumps, gonorrhea, HIV/AIDS, West-N:le virus; some disease state has vaccinated process using SVIR or SVEIR models, investigation of shigellosis and norovirus can use SEIAR model while smoking epidemic model using POSQL (the potential smoker, occasional smoker, smoker, temporarily quit smoker and permanently quit smoker) model. Over the years, more complex models have been derived. On the human population, the memory relates to the individual awareness [14]. In epidemic and endemic area's awareness about infection will lessen the contact rate between the different compartments such as human and the mosquitoes in dengue SIR-SI model [15,16], while the vaccinated people tend to have strong awareness of past epidemics, more than susceptible people in SVEIR model. There should be a scientific means to combine the models and observations such that experts will be able to extract as much information from available data as possible before making drastic decisions. Out of this overview, we refer to some obstacles in these models and takes a look at some intriguing approaches focusing on development of general structures for such models and proposes an alternative approach, namely fractional calculus, whose main features can be briefly summarized as follows: reflecting memory effects, capturing fractality, multiscale nature and better data fitting. The fractional derivative epidemic models provide a powerful instrument for incorporation of memory and hereditary properties of the systems as opposed to the integer order models, where such effects are neglected or difficult to incorporate. In addition, when fitting data, the fractional models has one more degree of freedom than the integer order model. We therefore, review several articles on fractional epidemic models and count models based on dynamics with derivative of fractional order and metapopulation models and propose that developing numerical techniques by which mathematical models are fitted to actual data can help guide the concerned bodies in preventing or controlling the infectious disease outbreaks.

In this paper, we mainly consider the fractional-order epidemic system with the fractional derivatives defined in Section 2 and introduce epidemiology modeling by formulating review in Section 3. Based on the numerical solution for the model review, we study the corresponding inverse problem of parameter estimation for the fractional differential equation by the novel techniques and optimization algorithm in Section 4 and 5. Then, we take the Norovirus infectious as an example about application to parameters estimation of fractional SEIAR model in Section 6 and propose a general multi-term fractional-order epidemic system with the new fractional orders and parameters in Section 7, for verifying the efficiency and accuracy of the proposed methods in dealing with the fractional inverse problem, a numerical example with experimental data is studied. Our general epidemic system is capable of providing numerical results that agree very well with the real data.

2. Preliminary knowledge

Fractional calculus is an old yet novel mathematical tool that unifies and generalises the derivative and integral of integer order into any arbitrary order. The theory of derivatives of non-integer order originated from the L'Hospital letter to Leibniz discussing the meaning of the derivative or what does the derivative of order $1/3$ or $\sqrt{2}$ of a function mean in 1695. Leading from that, it has caught the interest of mathematicians during 18th to 19th centuries to study this area. A well-known scientist, Abel in 1823 has become the first scientist to implicitly apply fractional calculus for investigating tautochrone problems. Later several fundamental works on various aspects of fractional calculus have appeared [17,18]. As one would expect, since fractional order differential equation systems allow greater degrees of freedom and incorporate memory effect in the model, they have become an excellent tool in modelling epidemiology properties and provide an interesting modeling technique in the context of epidemiology. Although the fractional derivative is more complicated than the classical model, there exist several numerical methods for solving such systems. Fractional calculus has been the subject of worldwide attention in the last decades [19], due to its broad range of applications in chemistry [20], biology [21–24], physics [25], engineering [26], viscoelastic materials [25], and image processing[27]. Recently, fractional calculus is experiencing an intensive progress in both theory and applications [28]. Fractional differential equations have been shown to be more adequate and can give a more realistic interpretation of natural phenomena than integer-order derivatives for describing phenomena associated with nonlocality, since the fractional-order derivative provides an excellent tool for the description of the memory and hereditary properties of various materials and processes [29]. Hence, fractional derivatives based on epidemic systems have also been used to deal with some epidemic behaviors [30–32]. The classical first-order differential equations was unable to reproduce the statistical data collected in a real outbreak of the disease with a sufficient degree of accuracy, in general, this basic/classical model does not provide enough good results. In order to have better results, that fit the reality, more specific and complicated set of differential equations have been investigated in the literature [33–35], we propose a slightly modified system of equations where we now use differential equations of fractional order.

Fractional SIR epidemic model equations are obtained from the classical SIR epidemic equations in mathematical modelling by replacing the first-order derivatives with fractional derivative of order $\alpha(0 < \alpha \leq 1)$. Several universal phenomena can be modeled to a great degree of accuracy by using the property of these evolution equations. In contrast to integer-order differential operators, which are local operators, a fractional-order differential operator is non-local in the sense that it takes into account the fact that the future state not only depends upon the present state but also on the history of its previous states. For this realistic property, the usage of fractional-order systems is becoming popular to model the behaviour of real systems in various fields of science and engineering. It is to be noted that the present states of any real-life dynamic system are dependent upon the history of its past states. Such circumstances have motivated the researchers to study the SIR epidemic model which has a great physical relevance from the perspective of public health policies and its consideration as fractional-order system in allied problems is valid [36].

In the recent years, the dynamic behaviors of fractional-order differential systems have received increasing attention. The existence of solutions of initial value problems for fractional order differential equations have been studied in the literature and the references there in [27,37–39]. Many definitions for fractional derivatives have been wildly studied. In this paper, we give three commonly used definitions: the Riemann-Liouville (RL), Caputo and the Grünwald-Letnikov (GL) definitions [29].

Definition 1. The fractional integral ${}_aD_t^{-\alpha}$ of function $f(t)$ is defined as follows:

$$ {}_aD_t^{-\alpha} f(t) = \frac{1}{\Gamma(\alpha)} \int_a^t (t-\tau)^{\alpha-1} f(\tau) d\tau, \tag{1} $$

where the fractional order $\alpha > 0$ and $\Gamma(z) = \int_0^\infty t^{z-1} e^{-t}\, dt$ is the gamma function.

Definition 2. The Caputo derivative with order α of function $f(t)$ is given as

$$ {}_a^C D_t^{\alpha} f(t) = {}_0D_t^{-(n-\alpha)} \frac{d^n}{dt^n} f(t) = \frac{1}{\Gamma(n-\alpha)} \int_a^t (t-\tau)^{n-\alpha-1} f^{(n)}(\tau) d\tau, \tag{2} $$

where $n-1 < \alpha < n,\ n \in Z^+$.

Definition 3. The Riemann-Liouville derivative with order α of function $f(t)$ is defined as

$$ {}_a^{RL} D_t^{\alpha} f(t) = \frac{d^n}{dt^n}\ {}_aD_t^{-(n-\alpha)} f(t) = \frac{1}{\Gamma(n-\alpha)} \frac{d^n}{dt^n} \int_a^t (t-\tau)^{n-\alpha-1} f(\tau) d\tau, \tag{3} $$

where $n-1 < \alpha < n,\ n \in Z^+$.

It follows from the definitions of fractional derivatives that the Riemann-Liouville and Caputo definition are not equivalent, and their relation is expressed by the following:

$$ {}_a^C D_t^{\alpha} f(t) = {}_a^{RL} D_t^{\alpha} f(t) - \sum_{k=0}^{n-1} \frac{(t-a)^{k-\alpha} f^{(k)}(a)}{\Gamma(k-\alpha+1)}. \tag{4} $$

The Caputo derivative is equivalent to the Riemann-Liouville derivative if the initial conditions $f^{(k)}(a) = 0,\ k = 0, 1, \cdots, n-1$.

Definition 4. The Grünwald-Letnikov derivative with order α of function $f(t)$ is defined as follows:

$$ \begin{aligned} {}_a^{GL} D_t^{\alpha} f(t) &= \lim_{\substack{h \to 0 \\ mh = t}} h^{-\alpha} \sum_{r=0}^{m} (-1)^r \binom{\alpha}{r} f(t - rh) \\ &= \sum_{k=0}^{n-1} \frac{f^{(k)}(a) t^{k-\alpha}}{\Gamma(k+1-\alpha)} + \frac{1}{\Gamma(n-\alpha)} \int_a^t (t-\tau)^{n-\alpha-1} f^{(n)}(\tau) d\tau, \end{aligned} \tag{5} $$

where $n-1 < \alpha < n$.

It follows from the definitions of fractional derivatives that the Grünwald-Letnikov fractional derivatives and Riemann-Liouville derivatives are equivalent. The Riemann-Liouville and Caputo definition are not equivalent, and their relation can be expressed by

$$ {}_a^C D_t^{\alpha} f(t) = {}_a^{RL} D_t^{\alpha} f(t) - \sum_{k=0}^{n-1} \frac{(t-a)^{k-\alpha} f^{(k)}(a)}{\Gamma(k-\alpha+1)} = {}_a^{RL} D_t^{\alpha} \left[f(t) - \sum_{k=0}^{n-1} \frac{(t-a)^k f^{(k)}(a)}{k!} \right], \tag{6} $$

Due to the relation (6), the Caputo derivative is equivalent to the Riemann-Liouville derivative if the initial conditions satisfy $f^{(k)}(a) = 0, k = 0, 1, \cdots, n-1$.

3. Model formulation review

3.1. Mathematical modeling of dengue epidemics (SIR-SI MODEL)

This global pandemic is attributed to the unprecedented population growth, the rising level of urbanization without adequate domestic water supplies, increasing movement of the virus between humans (due to tourism, migration, or international trade), and lack of effective mosquito control [40]. Dengue virus is transmitted to humans through the bite of infected Aedes mosquitoes, specially Aedes Aegypti. Once infected, a mosquito remains infected for life, transmitting the virus to susceptible individuals during feed. Dengue fever is a disease that has been found to cause problems whose magnitude has increased dramatically over the last two decades. In fact, the World Health Organization recently stated that it is the most important arthropod-borne viral disease of humans [41]. Therefore, it is very important to have a detailed understanding of the rules that the spread of the infection follows, so that the control of the vectors is the only possible strategy to combat the disease at the moment. More recent models indicate that in the coming decades the vectors transmitting the disease are likely to spread to even larger parts of the world, including most of central and even northern Europe. Some mathematical models have been proposed to study the outbreak of dengue fever. Nishiura [42] studied the mathematical and statistical analyses of the spread of dengue. Hales et al. [43] studied the global distribution of dengue fever on the basis of vapor pressure, which is a measure of humidity. Rodrigues et al. [44] studied the stability of the classic dengue disease model. Sardar [45] proposed a mathematical model of dengue transmission with memory. Pooseh et al. [46] studied the fractional-order dengue system with Riemann-Liouville-type derivatives of the same order. Diethelm [47] proposed a fractional-order model based on the Caputo-type derivative for the simulation of an outbreak of dengue fever, in which some orders are the same. However, in these papers, the parameters of the dengue model are given directly. In some papers, the numerical solution of these systems only provides a poor match with the real number of the infected humans.

In [46], the researchers assumed that the host population is divided into three classes: susceptible, $S_h(t)$, individuals who can contract the disease; infected, $I_h(t)$, individuals capable of transmitting the disease to others; and resistant, $R_h(t)$, individuals who have acquired immunity at time t. The total number of hosts is constant, i.e., $N_h = S_h(t) + I_h(t) + R_h(t)$. Similarly, they also have two compartments for the mosquito: $S_m(t)$ and $I_m(t)$ with $N_m = S_m(t) + I_m(t)$. The model is described by the system of differential equations

$$\begin{aligned}
\frac{dS_h(t)}{dt} &= \mu_h N_h - (B\beta_m h\frac{I_m}{N_h} + \mu_h)S_h,\\
\frac{dI_h(t)}{dt} &= B\beta_m h\frac{I_m}{N_h}S_h - (\eta_h + \mu_h)I_h,\\
\frac{dR_h(t)}{dt} &= \eta_h I_h - \mu_h R_h,\\
\frac{dS_m(t)}{dt} &= \mu_m N_m - (B\beta_h m\frac{I_h}{N_h} + \mu_m)S_m,\\
\frac{dI_m(t)}{dt} &= B\beta_h m\frac{I_h}{N_h}S_m - \mu_m I_m.
\end{aligned} \tag{7}$$

A particular feature of this system can be observed that

$$\frac{dN_h}{dt} = \frac{dS_h}{dt} + \frac{dI_h}{dt} + \frac{dR_h}{dt} = \mu_h(N_h - S_h - I_h - R_h) = 0, \tag{8}$$

i.e., the total number of humans is constant. This fact reflects the observation that indeed the number of people dying from dengue fever is extremely small. For example, in the outbreak considered below, less than 0.035% of the infected people eventually died from the disease. Similarly,

$$\frac{dN_m}{dt} = \frac{dS_m}{dt} + \frac{dI_m}{dt} = A - \mu_m(S_m + I_m) = A - \mu_m N_m, \tag{9}$$

where A is a constant recruitment rate for the mosquitoes. Subject to given initial conditions $S_h(0)$, $I_h(0)$, $R_h(0)$, $S_m(0)$ and $I_m(0)$. The recruitment rate of human and vector populations are denoted as $\mu_h N_h$ and $\mu_m N_m$, respectively. The natural death rate for humans and mosquitoes is described by the parameters μ_h and μ_m, respectively. They assumed that B is the average daily biting (per day) of the mosquito whereas $\beta_m h$ and $\beta_h m$ are related to the transmission probability (per bite) from infected mosquitoes to humans and vice versa. The recovery rate of the human population is denoted by η_h. Therefore, substitute the first-order derivatives by Riemann-Liouville derivatives of order α we have:

$$\begin{aligned}
{}_0^{RL}D_t^{\alpha} S_h(t) &= \mu_h N_h - (B\beta_m h\frac{I_m}{N_h} + \mu_h)S_h,\\
{}_0^{RL}D_t^{\alpha} I_h(t) &= B\beta_m h\frac{I_m}{N_h}S_h - (\eta_h + \mu_h)I_h,\\
{}_0^{RL}D_t^{\alpha} R_h(t) &= \eta_h I_h - \mu_h R_h,
\end{aligned} \tag{10}$$

$$
\begin{aligned}
{}_0^{RL}D_t^{\alpha} S_m(t) &= \mu_m N_m - \left(B\beta_h m \frac{I_h}{N_h} + \mu_m\right) S_m, \\
{}_0^{RL}D_t^{\alpha} I_m(t) &= B\beta_h m \frac{I_h}{N_h} S_m - \mu_m I_m.
\end{aligned}
$$

Note that the fractional system reduces to classical system if $\alpha \to 1$. Researchers used classical methods to obtain an approximate solution to the original fractional system and solved numerically using data that outbreak occurred in 2009 in Cape Verde and concluded the best order is 0.987, as the percentage error is thirteen as compared to classical model is sixty two [46].

In 2013, the researchers assumed that mosquitoes and humans behave in a different way and used two different orders of the differential operators, α_h and α_m [47]. They first replaced the fractional calculus system using fractional Caputo derivatives as following [47]:

$$
\begin{aligned}
{}_0^{C}D_a^{\alpha_h} S_h &= \mu_h(N_h - S_h) - \frac{\beta_h b}{N_h} S_h I_m, \\
{}_0^{C}D_a^{\alpha_h} I_h &= \frac{\beta_h b}{N_h} S_h I_m - (\mu_h + \gamma) I_h, \\
{}_0^{C}D_a^{\alpha_h} R_h &= \gamma I_h - \mu_h R_h, \\
{}_0^{C}D_a^{\alpha_m} S_m &= \mu_m N_m - \frac{\beta_m b}{N_h} S_m I_h - \mu_m S_m, \\
{}_0^{C}D_a^{\alpha_m} I_m &= \frac{\beta_m b}{N_h} S_m I_h - \mu_m I_m.
\end{aligned}
\tag{11}
$$

To make sure that the right-hand sides of these equations have same dimensions, they modified the right-hand sides to make the dimensions match as following [47]:

$$
\begin{aligned}
{}_0^{C}D_a^{\alpha_h} S_h &= \mu_h^{\alpha_h}(N_h - S_h) - \frac{\beta_h b^{\alpha_h}}{N_h} S_h I_m, \\
{}_0^{C}D_a^{\alpha_h} I_h &= \frac{\beta_h b^{\alpha_h}}{N_h} S_h I_m - (\mu_h^{\alpha_h} + \gamma^{\alpha_h}) I_h, \\
{}_0^{C}D_a^{\alpha_h} R_h &= \gamma^{\alpha_h} I_h - \mu_h^{\alpha_h} R_h, \\
{}_0^{C}D_a^{\alpha_m} S_m &= \mu_m^{\alpha_m} N_m - \frac{\beta_m b^{\alpha_m}}{N_h} S_m I_h - \mu_m^{\alpha_m} S_m, \\
{}_0^{C}D_a^{\alpha_m} I_m &= \frac{\beta_m b^{\alpha_m}}{N_h} S_m I_h - \mu_m^{\alpha_m} I_m.
\end{aligned}
\tag{12}
$$

The authors numerically simulated using Adams method and used the data based on the 2009 dengue fever outbreak in Cape Verde islands. It can be clearly seen that both fractional models provide almost identical results up to the peak of the number of infected humans whereas the later phase of the epidemic is more accurately modeled by the system using the modified parameters. The authors have demonstrated that a nonlinear fractional order differential equation model can simulate the dynamics of the epidemic much more accurately than the classical model based on first derivatives. In particular, it has turned out that the behavior of the human population follows a model of a different order than the mosquito population.

In 2019, the researchers proposed a new and general fractional-order dengue fever system using Caputo derivatives with different orders [48]:

$$
\begin{aligned}
\lambda_{\alpha_1}\, {}_0^{C}D_t^{\alpha_1} S_h &= \mu_h(N_h - S_h) - \frac{\beta_h b}{N_h + m} S_h I_m, \\
\lambda_{\alpha_2}\, {}_0^{C}D_t^{\alpha_2} I_h &= \frac{\beta_h b}{N_h + m} S_h I_m - (\mu_h + \gamma) I_h, \\
\lambda_{\alpha_3}\, {}_0^{C}D_t^{\alpha_3} R_h &= \gamma I_h - \mu_h R_h, \\
\lambda_{\alpha_4}\, {}_0^{C}D_t^{\alpha_4} S_m &= \mu_m(N_m - S_m) - \frac{\beta_m b}{N_h} S_m I_h, \\
\lambda_{\alpha_5}\, {}_0^{C}D_t^{\alpha_5} I_m &= \frac{\beta_m b}{N_h + m} S_m I_h - \mu_m I_m,
\end{aligned}
\tag{13}
$$

where ${}_0^{C}D_t^{\alpha_i}$ denotes the Caputo fractional derivative with order α_i. For searching a better dengue fever system which is capable of providing numerical results that agree much better with the real data, they present the multi-term fractional order dengue model as follows [48]:

$$
{}_0^{C}D_t^{\alpha_1,\cdots,\alpha_r,\alpha_0} S_h = \mu_h(N_h - S_h) - \frac{\beta_h b}{N_h + m} S_h I_m,
$$

$$
\begin{aligned}
{}_0^C D_t^{\alpha_1,\cdots,\alpha_r,\alpha_0} I_h &= \frac{\beta_h b}{N_h + m} S_h I_m - (\mu_h + \gamma) I_h, \\
{}_0^C D_t^{\alpha_1,\cdots,\alpha_r,\alpha_0} R_h &= \gamma I_h - \mu_h R_h, \\
{}_0^C D_t^{\beta_1,\cdots,\beta_r,\beta_0} S_m &= \mu_m (N_m - S_m) - \frac{\beta_m b}{N_h} S_m I_h, \\
{}_0^C D_t^{\beta_1,\cdots,\beta_r,\beta_0} I_m &= \frac{\beta_m b}{N_h + m} S_m I_h - \mu_m I_m,
\end{aligned} \tag{14}
$$

where the ${}_0 D_t^{\alpha_1,\cdots,\alpha_r,\alpha_0}$ and ${}_0 D_t^{\beta_1,\cdots,\beta_r,\beta_0}$ are defined as

$$
{}_0^C D_t^{\alpha_1,\cdots,\alpha_r,\alpha_0} x(t) = \sum_{i=1}^{r} \lambda_i \cdot {}_0 D_t^{\alpha_i} x(t) + \lambda_0 \cdot {}_0 D_t^{\alpha_0} x(t), \tag{15}
$$

and

$$
{}_0^C D_t^{\beta_1,\cdots,\beta_r,\beta_0} x(t) = \sum_{i=1}^{r} \lambda_i' \cdot {}_0 D_t^{\beta_i} x(t) + \lambda_0' \cdot {}_0 D_t^{\beta_0} x(t), \tag{16}
$$

with $0 < \alpha_1 < \cdots < \alpha_r < \alpha_0 = 1$, $0 < \beta_1 < \cdots < \beta_r < \beta_0 = 1$, and the weighted coefficient λ_i, $\lambda_i (i = 1, 2, \cdots, r) \in R^+$ which are used to retain the same units on both sides of the equations.

To verify the effectiveness and correctness of the proposed methods, they used the data of 2009 dengue fever outbreak on the Cape Verde island given by Diethelm as the known data to perform the inverse problem by parameter estimation method [48]. They studied the effect of every parameter on the number of infected humans with the other parameters fixed. The results showed a better fitting between the numerical solutions of the multi-term fractional-order dengue fever model with the estimated parameter values and the real data than other models. Hence, this paper provides effective parameter estimation methods for a fractional application in the dengue fever model.

In [49], a study on a basic fractional order epidemic model of dengue transmission is conducted using the SIR-SI model, including the aquatic phase of the vector. In the formulation of the model, the total number of human and mosquito population is assumed to be constant. Assumed that the infection is produced by only one serotype of dengue viruses. The dynamics of female Aedes mosquito includes aquatic phase, A_m, and adult mosquito stage. The adult stage is divided into two compartments which are susceptible M_s and infectious M_i. The total human population is partitioned into three compartments that are susceptible H_s, infectious H_i, and recovered H_r individuals. The fractionalization is done following the work of Diethelm [47]. The governing equation is as follows:

$$
\begin{aligned}
{}_0^C D_t^{\alpha} A_m &= q\phi (1 - \frac{A_m}{C}) M - (\sigma_A + \mu_A) A_m, \\
{}_0^C D_t^{\alpha} M_s &= \sigma_A A_m - \frac{b^{\alpha} \beta_m}{H} M_s H_i - \mu_m M_s, \\
{}_0^C D_t^{\alpha} M_i &= \frac{b^{\alpha} \beta_m}{H} M_s H_i \mu_m M_i, \\
{}_0^C D_t^{\alpha} H_s &= \mu_h (H - H_s) - \frac{b^{\alpha} \beta_h}{H} H_s M_i, \\
{}_0^C D_t^{\alpha} H_i &= \frac{b^{\alpha} \beta_h}{H} H_s M_i - (\gamma_h + \mu_h) H_i, \\
{}_0^C D_t^{\alpha} H_r &= \gamma_h H_i - \mu_h H_r,
\end{aligned} \tag{17}
$$

with the condition of $N_h = H = H_s + H_i + H_r$, we have $H_r = H - H_s + H_i$. Thus, the authors wrote down the corresponding system for human population exclusive of the H_r differential equation as follows [49]:

$$
\begin{aligned}
{}_0^C D_t^{\alpha} H_s &= \mu_h (H - H_s) - \frac{b^{\alpha} \beta_h}{H} H_s M_i, \\
{}_0^C D_t^{\alpha} H_i &= \frac{b^{\alpha} \beta_h}{H} H_s M_i - (\gamma_h + \mu_h) H_i, \\
{}_0^C D_t^{\alpha} A_m &= q\phi (1 - \frac{A_m}{C}) M - (\sigma_A + \mu_A) A_m, \\
{}_0^C D_t^{\alpha} M_s &= \sigma_A A_m - \frac{b^{\alpha} \beta_m}{H} M_s H_i - \mu_m M_s, \\
{}_0^C D_t^{\alpha} M_i &= \frac{b^{\alpha} \beta_m}{H} M_s H_i \mu_m M_i.
\end{aligned} \tag{18}
$$

In this study [49], the values related to the human describe the reality of an infected period in Malaysia. The data used is based on the dengue fever cases recorded in Malaysia for 2016, taken from The Ministry of Health Malaysia. Table 1 summarised the fractional-order dengue epidemics models and the contribution to the research works in recent years.

Table 1
Summary of dengue epidemics models.

Year	Author	Model	Contribution
2011	Pooseh et al. [46]	fractional-order SIR-SI model with Riemann-Liouville derivatives of the same order	The best order α is 0.987. The percentage error is 13 as compared to classical model is 62.
2013	Diethelm et al. [47]	fractional-order SIR-SI model with Caputo derivatives of two different orders	A particularly good approximation was obtained with $\alpha_h = 1$ and $\alpha_m \in [0.75, 0.8]$. The improved simulation results by setting $\alpha_m = 0.95$ and $\mu_m = 0.196$.
2014	Al-Sulami et al. [50]	fractional-order SIR-SI model with Caputo derivatives of the same order	It very sensitive to the order of differentiation α: a small change in α may result in a big change.
2015	T. Sardar et al. [14]	fractional-order SIR-SI model with Caputo derivatives of two different orders considering the dimension match of the system	Increase in human memory ($\alpha \to 0$) will reduce the dengue transmission; Increase in memory of vectors ($\beta \to 0$) will increase the dengue transmission.
2018	Hamdan et al. [51]	fractional-order SI-SIR model with Caputo derivatives by including the aquatic stages	DFE is locally asymptotically stable when $R_0 < 1$ and is unstable when $R_0 > 1$.
2019	Hamdan et al. [49]	fractional-order SIR-SI model using Caputo derivatives including aquatic phase	The disease-free equilibrium of system is locally asymptotically stable if the corresponding $R_0 < 1$
2019	T. Li et al. [48]	fractional-order SIR-SI model using Caputo derivatives with different orders	A better fitting between the numerical solutions of the multi-term fractional-order dengue model with the estimated parameter values and the real data than other models.
2020	Ozlem Defterli[52]	Fractional-order vector-host dengue model using Caputo derivatives by including temperature dependent features in entomological parameters.	Stability analysis is performed and the local asymptotic stability of the disease-free equilibria is obtained. The highest danger of dengue transmission exists at temperature $28^{\circ}C$.

3.2. Mathematical modeling of leptospirosis epidemics (SIR-SI MODEL)

Leptospirosis disease is an important infectious disease. This kind of infection occurs in urban areas of industrialized and developed countries and also in the rural areas. The people of the city who walk in dirty water are mostly infected. Workers planting rice, sewer cleaners, cleaning canals workers, and agriculture labor get the disease easily. The disease flourishes due to delay in diagnosis and unavailability of clinical infrastructure. The cause of the disease is bacteria. It is potentially fatal infection of brain, kidney, liver, heart, and lung. The people who can get infection are those who have contact with infected animals, soil, or water in which the bacteria is present. The outdoor people, who work with animals, face the risk of leptospirosis infection, similarly workers in farms, sewer, mine, slaughter houses, dairy farmers, and animal caretakers and those who work with fishes and military personnel. Those people who work outdoors like swimming, rafting, and kayaking also face the risk of infection.

The researchers had made many efforts for modeling of leptospirosis epidemic disease since 2011 [53–58]. They proposed a mathematical model that describes the epidemic leptospirosis disease given by:

$$\begin{aligned}
\frac{dS^h(t)}{dt} &= b_1 - \mu_h S^h - \beta_2 S^h I^v - \beta_1 S^h I^h + \lambda_h R^h,\\
\frac{dI^h(t)}{dt} &= \beta_2 S^h I^v + \beta_1 S^h I^h - (\mu_h + \delta_h + \gamma_h) I^h,\\
\frac{dR^h(t)}{dt} &= \gamma_h I^h - \mu_h R^h - \lambda_h R^h,\\
\frac{dS^v(t)}{dt} &= b_2 - \gamma_v S^v - \beta_3 S^v I^h,\\
\frac{dI^v(t)}{dt} &= \beta_3 S^v I^h - (\gamma_v + \delta_v) I^v,
\end{aligned} \tag{19}$$

where $S^h(t)$, $I^h(t)$, $R^h(t)$, $S^v(t)$ and $I^v(t)$ represent the population of susceptible human, infected human, recovered human, susceptible vector, and infected vector at time t, respectively. The rate at which the population of human increases is shown by b_1. The natural mortality rate for the human population is μ_h; β_1, β_2, and β_3 represent the transmission coefficients. The parameter λ_h shows the individuals who become susceptible again. The death from the disease that occurs to humans is shown by δ_h. The rate of recovery from infection for the human is denoted by γ_h. The growth rate of the vector population is represented by b_2; γ_v is the natural death rate for vector and disease related death rate for the vector is δ_v. The fractional model presented by [54] is given by system above which represents a system of nonlinear ODE and is given as follows:

$$\begin{aligned}
{}_0^C D_t^\alpha S^h(t) &= b_1 - \mu_h S^h - \beta_2 S^h I^v - \beta_1 S^h I^h + \lambda_h R^h,\\
{}_0^C D_t^\alpha I^h(t) &= \beta_2 S^h I^v + \beta_1 S^h I^h - (\mu_h + \delta_h + \gamma_h) I^h,\\
{}_0^C D_t^\alpha R^h(t) &= \gamma_h I^h - \mu_h R^h - \lambda_h R^h,
\end{aligned} \tag{20}$$

$$
\begin{aligned}
{}_0^C D_t^{\alpha} S^v(t) &= b_2 - \gamma_v S^v - \beta_3 S^v I^h,\\
{}_0^C D_t^{\alpha} I^v(t) &= \beta_3 S^v I^h - (\gamma_v + \delta_v) I^v.
\end{aligned}
$$

The parameter which describes the general response expression in representing the order of fractional derivative gives different results for different values. Obviously, the integer-order system can be viewed as a special case of the fractional-order system by putting the time-fractional order of the derivative equal to one. To put it simple, for the higher in order, the behavior of the fractional order system is the same in the case of integer order. This is the first work, which is available on the epidemic model of leptospirosis in fractional order. They solved the fractional systems and compared with classical Runge Kutta and concluded that the results obtained by multi-step generalized differential transform have a good agreement with the Runge Kutta of order 4 [59].

3.3. Mathematical modeling of salmonella bacterial infection epidemics(SIRC MODEL)

The Salmonella infection is a major zoonotic disease which is transmitted between humans and other animals. Most persons infected with Salmonella develop diarrhea, fever, and abdominal cramps 12 to 72 hours after infection. The illness usually lasts 4 to 7 days, and most persons recover without treatment. However, in some persons, the diarrhea may be so severe that the patient needs to be hospitalized. Salmonella live in The intestinal tracts of humans and other animals, including birds. Salmonella are usually transmitted to humans by eating foods contaminated with animal feces. Contaminated foods usually look and smell normal. Contaminated foods are often of animal origin, such as beef, poultry, milk, or eggs, but any food, including vegetables, may become contaminated. Therefore, Salmonella is considered as a serious problem for the public health throughout the world. There are no doubts that mathematical modeling of Salmonella bacterial infection plays an important role in gaining understanding of the transmission of the disease in specific environment and in predicting the behavior of any outbreak.

The researchers introduced a new compartment into SIR model, which is called cross-immune compartment to be called SIRC model [60]. The new compartment cross-immune describes an intermediate state between the fully susceptible and the fully protected one. Recently, the fractional order SIRC model of influenza, a disease in human population, was investigated [61]. The researchers considered the fractional order SIRC model associated with evolution of Salmonella bacterial infection in animal herds. However, they took into account the disease induced mortality rate in the model. Qualitative behavior of the fractional order SRIC model was investigated and numerical simulations of the fractional order SRIC model were provided to demonstrate the effectiveness of the proposed method by using implicit Euler's method.

In [62], the authors assumed that the Salmonella infection spreads in animal herds which are grouped as four compartments, according to their infection status: $S(t)$ is the proportion of susceptible individuals at time t (individuals that do not have the bacterial infection), $I(t)$ is the proportion of infected individuals (that have the bacterial infection), $R(t)$ is the proportion of recovered individuals (that recovered from the infection and have temporary immunity), and $C(t)$ is the proportion of cross-immune individuals at time t. The total number of animals in the herd is given by $N = S + I + R + C$. They considered that initially all the animals are susceptible to the infection. Once infected, a susceptible individual leaves the susceptible compartment and enters the infectious compartment where it then becomes infectious. The infected animals pass into the recovered compartment. The individuals who have recovered from the disease have temporary immunity and grouped into $C(t)$ compartment. Therefore, the disease transmission model consists of nonnegative initial conditions together with system of equations as follows:

$$
\begin{aligned}
\frac{dS(t)}{dt} &= \mu N + \eta C(t) - (\beta I(t) + \mu) S(t),\\
\frac{dI(t)}{dt} &= \beta S(t) I(t) + \sigma \beta C(t) I(t) - (\theta + m + \mu) I(t),\\
\frac{dR(t)}{dt} &= (1-\sigma)\beta C(t) I(t) + \theta I(t) - (\mu + \delta) R(t),\\
\frac{dC(t)}{dt} &= \delta R(t) - \beta C(t) I(t) - (\eta + \mu) C(t),
\end{aligned}
\tag{21}
$$

where parameter μ denotes the mortality rate in every compartment and is assumed to be equal to the rate of newborns in the population. β is the contact rate and also called transmission from susceptible to infected. η^{-1} is the cross immune period, θ^{-1} is the infectious period, δ^{-1} is the total immune period, and σ is the fraction of the exposed cross immune individuals who are recruited in a unit time into the infective subpopulation [60], [63]. The disease induces mortality rate is noted by m.

Although a large number of work have been done in modeling the dynamics of epidemiological diseases, it has been restricted to integer-order (delay) differential equations. In recent years, it has turned out that many phenomena in different fields can be described very successfully by models using fractional order differential equations (FODEs). The author in [62] introduced fractional order into model aboved. They assumed that $s(t) = \frac{S(t)}{N}$, $i(t) = \frac{I(t)}{N}$, $r(t) = \frac{R(t)}{N}$, $c(t) = \frac{C(t)}{N}$, where N is the total number of population, and the fractional model takes the form as follows:

$$
{}_0^C D_t^{\alpha_1} s(t) = \mu + \eta c(t) - (\beta i(t) + \mu) s(t),
$$

$$
\begin{aligned}
{}_0^C D_t^{\alpha_2} i(t) &= \beta s(t) i(t) + \sigma \beta c(t) i(t) - (\theta + m + \mu) i(t), \\
{}_0^C D_t^{\alpha_3} r(t) &= (1-\sigma)\beta c(t) i(t) + \theta i(t) - (\mu + \delta) r(t), \\
{}_0^C D_t^{\alpha_4} c(t) &= \delta r(t) - \beta c(t) i(t) - (\eta + \mu) c(t).
\end{aligned} \tag{22}
$$

The researchers provided a fractional order SIRC epidemic model with Salmonella bacteria infection and derived the sufficient conditions to preserve the asymptotic stability of infection-free and endemic steady states. The fractional order dynamical models are more suitable to model biological systems with memory than their integer-orders and the presence of a fractional differential order into a corresponding differential equation leads to a notable increase in the complexity of the observed behavior and enlarges the stability region of the solutions.

3.4. Mathematical modeling of H1N1 epidemics(SEIR MODEL)

The pandemic virus A(H1N1)/09 is a flu virus of swine, avian, and human origin that was first identified in April 2009 in Mexico and the USA [64]. The virus soon spread to the rest of the world and on June 11, 2009; the WHO declared the new influenza A(H1N1) a pandemic [64]. The transmission of the virus AH1N1 is only possible through effective contacts of a susceptible individual with an infectious individual. Typical interventions to control the spread include quarantine, isolation, travel restrictions, closing of public places, fear-based self-quarantine, and cancelation of events [64]. These interventions have economic costs to individuals and society related to lost work, increased school absenteeism, and decreased business revenues [65,66]. A pandemic influenza A(H1N1) vaccine became available in the USA in October 2009 [67]. Every year, approximately 36,000 people die from seasonal influenza or flu-related causes only in the USA [67]. Additionally, since there are thousands deaths worldwide due to the A(H1N1)/09 virus, it is important to understand the dynamics regarding the evolution of the A(H1N1)/09 virus.

In order to study the dynamics of H1N1 influenza virus spread, several models have been presented. For instance, the classical SIR epidemiological model with a seasonal forced function has been used to model the influenza A(H1N1)/09 virus spread in the US population [68]. The classical SEIR model has been used to predict the infected individuals, hospital bed shortage, and effectiveness of vaccination in a city of Japan and mixed with statistical methods in order to forecast the prevalence of A(H1N1) in Singapore [65,69]. However, when considering influenza, the SEIR model, which is an immediate extension of the original SIR model, is more realistic. The SEIR model introduces a fourth compartment corresponding to the incubation (disease latency) stage when a person is infected but still not infectious enough to be able to transmit it. The SEIR model has been applied in epidemics that include a latency and recovery periods such dengue, influenza, rabies, and tuberculosis [44,70–73]. For instance, the SEIR model has been used to describe real data of tuberculosis, and the least squares fitting has been used for estimating the model parameters [72]. Furthermore, the SEIR model has been used to explore effective control and prevention measures for the human rabies in China, where it is one of the major public health problems [73].

In [74], the authors proposed the population scaled fractional SEIR using Caputo derivatives of order α. The proposed model was then fitted to the known real data related to H1N1 infected cases. The SEIR epidemiological model considers that the total population $N(t)$ is divided into four subpopulations: $S(t)$ susceptible, $E(t)$ people incubating the virus, infectious $I(t)$, and recovered $R(t)$ subpopulations. In addition, the newborn children become susceptible at a rate μ (birth rate), and individuals leave the system by death at a rate d. An individual in $S(t)$ flows to $E(t)$ because people in $I(t)$ transmit A(H1N1) virus by effective contacts at rate β. Finally, they consider that once an individual is recovered, he or she acquires permanent immunity [67]. The other parameters of the model are ρ, recovery rate from the infection and latent individuals become infected at rate Ω. The population-scaled SEIR model (without loss of generality) with constant population size ($d = \mu$) is given by [74]:

$$
\begin{aligned}
\frac{dS(t)}{dt} &= \mu - \beta S(t) I(t) - \mu S(t), \\
\frac{dE(t)}{dt} &= \beta S(t) I(t) - (\mu + \Omega) E(t), \\
\frac{dI(t)}{dt} &= \Omega E(t) - (\mu + \rho) I(t), \\
\frac{dR(t)}{dt} &= \rho I(t) - \mu R(t).
\end{aligned} \tag{23}
$$

Then, the authors considered the SEIR fractional model using Caputo derivatives of order α as follows [74]:

$$
\begin{aligned}
{}_0^C D_t^{\alpha} S(t) &= \mu^{\alpha} - \beta^{\alpha} S(t) I(t) - \mu^{\alpha} S(t), \\
{}_0^C D_t^{\alpha} E(t) &= \beta^{\alpha} S(t) I(t) - (\mu^{\alpha} + \Omega^{\alpha}) E(t), \\
{}_0^C D_t^{\alpha} I(t) &= \Omega^{\alpha} E(t) - (\mu^{\alpha} + \rho^{\alpha}) I(t), \\
{}_0^C D_t^{\alpha} R(t) &= \rho^{\alpha} I(t) - \mu^{\alpha} R(t).
\end{aligned} \tag{24}
$$

In the fractional model, the next state depends not only upon its current state but also upon all of its historical states. The authors tested the proposed SEIR fractional order model with real data. The parameter values of the model were esti-

mated minimizing the mean square error between the fractional model outputs and the real data of influenza A(H1N1). The proposed fractional model epidemic peak adjusts better to the peak of the real data and gives better results in terms of the mean square error then with the classical SEIR model. This fact is important from a health point of view since it translates to a longer period with a high number of infected individuals, which can affect the health system. It is concluded that the fractional order epidemic model produces numerical results that agree very well with the real data of influenza A(H1N1) and provides useful information for the understanding, prediction, and control of the transmission of different epidemics are in many cases a more powerful approach to epidemiological models, because one can choose the order α of fractional differentiation that best corresponds to real data.

3.5. Mathematical modeling of measles epidemics(SEIR MODEL)

Measles is a higher contagious viral disease caused by infection of Paramyxovirus, generally of the genus Morbillivirus. It is a serious disease of childhood that can lead to complications and death. For example, measles caused about 7500 deaths in the United States in 1920 and still causes about 1 million deaths worldwide each year [75]. Measles vaccinations are given to children between 6 and 18 months of age, but the optimal age of vaccination for measles seems to vary geographically. Its incubation period is located somewhere between 9 and 12 days and its infectivity period between 4 and 9 days. Measles is highly present in early childhood and its epidemics are commonly related to aggregation of children at schools or child-care centres. It is recommended to get vaccinated against it at around 18 months of age and have a booster at 4 to 5 years of age. The disease is particularly characterized by its low mortality and high morbidity. Measles will continue to circulate in a community with a higher number of susceptible hosts by birth of children. However, in communities which generate insufficient new hosts, measles will die out. This theory was introduced in 1957 by Bartlett [76], who brought out the critical population size for a community and referred it to be the minimum number supporting measles.

In [77], the authors formulated the system modeling the fractional temporal spread of measles in a human population. In the model, a population supposed constant is divided into different classes, disjoint and based on their disease status. At time t, $S = S(t)$ is the fraction of population representing individuals susceptible to measles, $E = E(t)$ is the fraction of population representing individuals exposed to measles, $I = I(t)$ is the fraction of population representing individuals infectious with measles, and $R = R(t)$ is the fraction of population representing individuals that recovered from measles. They assumed that all recruitment is done by birth into the class of susceptible and occurs at constant birth rate b. The rate constant for nondisease related death is μ; thus $\frac{1}{\mu}$ is the average lifetime. They used the standard mass balance incidence expressions $\beta(t)SI$ to indicate successful transmission of measles due to effective contacts dynamics in the population by infectious individuals. Once infected, a fraction of exposed people becomes infectious with a constant rate σ, so that $\frac{1}{\sigma}$ is the average incubation period. Some infectious individuals will recover after a treatment or a certain period of time at a rate constant ζ, making $\frac{1}{\zeta}$ the average infectious period. The formulated fractional temporal SEIR measles model is given by [77]:

$$\begin{aligned} {}_0^C D_t^\alpha S &= b - (\beta(t)I + \mu)S, \\ {}_0^C D_t^\alpha E &= \beta(t)SI - (\sigma + \mu)E, \\ {}_0^C D_t^\alpha I &= \sigma E - (\zeta + \mu)I, \\ {}_0^C D_t^\alpha R &= \zeta I - \mu R. \end{aligned} \tag{25}$$

This model was solved by predictor corrector scheme of Adams Bashforth Moulton type [77]. The authors had started by showing nonnegativity of solutions to the fractional metapopulation model which defined as system of differential equations generated by discrete spatial models with continuous time and have been thoroughly analyzed in numeral articles [78,79] thereby addressing the problem of its well posedness. They had also shown that the disease-free equilibrium of the model is linearly stable if the spectral radius (the basic reproduction number) $R_0 \leq 1$ and unstable if $R_0 \geq 1$. They simulated numerical data based on online magazine Otago Daily Time. Numerical simulations shown that, even in fractional dynamics of measles in metapopulation, the epidemic will not occur in communities which generate insufficient new hosts, which is in accordance with the theory of Bartlett. This work generalizes the preceding ones with the inclusion of the fractional dynamics to a combined SEIR and metapopulation model, giving at the same time one of the multiple applications of fractional differential equations.

In 2018, a fractional temporal SEIR measles mode was considered. The model consists of four coupled time fractional ordinary differential equations. The time-fractional derivative is defined in the Caputo sense. In this model, the population is spatially spread into four patches representing four cities. The authors considered the set $\mathbb{P} = \{A, B, W, D\}$ representing four patches. The m_{xy}^c is the rate of travel from city x to city y in compartment c with $c = S, E, I, R$ which represents the transfer rate of individuals in the compartment c of city x moving to the same compartment c in city y. It is clear that $m_{xx}^c = 0$, for all $x \in \mathbb{P}$ and $c \in \{S, E, I, R\}$. The basic metapopulation model is given by [80]

$$\begin{aligned} \frac{dS_x}{dt} &= b_x - (\beta_x(t)I_x + \mu_x)S_x + \sum_{y\in\mathbb{P}} S_y m_{yx}^S - S_x \sum_{y\in\mathbb{P}} m_{xy}^S, \\ \frac{dE_x}{dt} &= \beta_x(t)S_x I_x - (\sigma_x + \mu_x)E_x + \sum_{y\in\mathbb{P}} E_y m_{yx}^E - E_x \sum_{y\in\mathbb{P}} m_{xy}^E, \end{aligned} \tag{26}$$

$$\frac{dI_x}{dt} = \sigma_x E_x - (\xi_x + \mu_x)I_x + \sum_{y\in\mathbb{P}} I_y m^I_{yx} - I_x \sum_{y\in\mathbb{P}} m^I_{xy},$$
$$\frac{dR_x}{dt} = \xi_x I_x - \mu_x R_x + \sum_{y\in\mathbb{P}} R_y m^R_{yx} - R_x \sum_{y\in\mathbb{P}} m^R_{xy}.$$

The fractional temporal model is formulated by the following differential equations with the fractional derivative in the sense of Caputo.

$$\begin{aligned}
{}^C_0D^\alpha_t S_x &= b_x - (\beta_x(t)I_x + \mu_x)S_x + \sum_{y\in\mathbb{P}} S_y m^S_{yx} - S_x \sum_{y\in\mathbb{P}} m^S_{xy},\\
{}^C_0D^\alpha_t E_x &= \beta_x(t)S_x I_x - (\sigma_x + \mu_x)E_x + \sum_{y\in\mathbb{P}} E_y m^E_{yx} - E_x \sum_{y\in\mathbb{P}} m^E_{xy},\\
{}^C_0D^\alpha_t I_x &= \sigma_x E_x - (\xi_x + \mu_x)I_x + \sum_{y\in\mathbb{P}} I_y m^I_{yx} - I_x \sum_{y\in\mathbb{P}} m^I_{xy},\\
{}^C_0D^\alpha_t R_x &= \xi_x I_x - \mu_x R_x + \sum_{y\in\mathbb{P}} R_y m^R_{yx} - R_x \sum_{y\in\mathbb{P}} m^R_{xy}.
\end{aligned} \tag{27}$$

where Γ is the Gamma function. This fractional measles model was used to construct the analytical technique and predictor-corrector scheme. The authors also explored the average error estimates for the measles model to verify with the theoretical analysis. They used the GMMP scheme (Gorenflo-Mainardi-Moretti-Paradisi) [81] to show the accuracy of the analytical solution for the time coupled fractional differential equations. The best features of the techniques proposed in this work are that they can be easily extended to other fractional epidemic models. The authors limited the discussions on the effect of differential order but put more effort into constructing a simple and effective analytical technique that can be easily applied to other fractional models. In some circumstances, the solutions from the derived techniques can also help to understand the underlying mechanisms that influence the epidemic pattern. It can be concluded that the analytical technique presented in this paper is reliable and yet an alternative for the analytical evaluation to other time fractional differential equations models.

3.6. Mathematical modeling of an anti-SARS vaccine (SVEIR MODEL)

The World Health Organization (WHO) reported the emergence of a new respiratory disease known as severe acute respiratory syndrome (SARS) in March 2003. The disease, caused by a coronavirus, spread rapidly across Asia, Europe and North America, with the highest prevalence in Asia. SARS resulted in about 900 deaths and 8000 infections globally.

Owing to the rapid transmissibility of the virus and the fear of a large epidemic, the WHO spearheaded an international effort to combat the spread of SARS. Absent a definitive anti-SARS treatment or vaccine, these efforts were based on the quarantine of suspected cases and isolation of individuals infected with SARS-CoV to stop them from infecting others. Many advances have been made towards the design of a vaccine for SARS, and some vaccines are undergoing clinical trials. This is a welcome development since, historically, vaccines have been and continue to be very useful in preventing illness or death of millions of individuals.

Over the past few decades, a large number of simple compartmental mathematical models of the general form SVI or SVIR (where S, V, I and R denote the populations of susceptible, vaccinated, infectious and recovered individuals) have been used in the literature to assess the impact or potential impact of imperfect vaccines for combatting the spread of some human diseases. While in some of these studies the vaccine is only given to people newly recruited into the population, such as newborns (cohort vaccination), in many others, a proportion of susceptible individuals is continuously vaccinated. In other studies, such as Arino et al. [82], both cohort and continuous vaccination are provided. Gandon et al. [83] provided a nice study on some of the epidemiological and evolutionary consequences associated with the use of imperfect vaccines using an SVI model with two infected components (unvaccinated infected and vaccinated infected individuals). Their study, which is based on an imperfect vaccine which may decrease probability of infection and/or may decrease the growth rate of parasites within the host, shows that eradication success depends on the type of vaccine and vaccine coverage used. The model constructed in the current paper is an extension of the standard SVIR models, including a new compartment for the latent class (an essential feature of the SARS transmission dynamics).

The development of the mathematical model in [84] is based on subdividing a given SARS-affected community into five compartments: susceptible, $S(t)$, vaccinated, $V(t)$, asymptomatic, $E(t)$, symptomatic, $I(t)$, and recovered, $R(t)$, individuals. The total population size is $N(t) = S(t) + V(t) + E(t) + I(t) + R(t)$. The rates of change of the populations in each compartment are represented by the following equations:

$$\frac{dS}{dt} = \Pi - \beta SI - \xi S - \mu S,$$
$$\frac{dV}{dt} = \xi S - (1-\tau)\beta VI - \mu V,$$

$$\begin{aligned}
\frac{dE}{dt} &= \beta SI + (1-\tau)\beta VI - \alpha E - \mu E, \\
\frac{dI}{dt} &= \alpha E - \delta I - dI - \mu I, \\
\frac{dR}{dt} &= \delta I - \mu R.
\end{aligned} \tag{28}$$

In [85], Wei et al. proposed a new SVEIR epidemic disease model with time delay

$$\begin{aligned}
\frac{dS}{dt} &= \mu - \mu S(t) - \beta S(t)I(t), \\
\frac{dV}{dt} &= -\beta_1 V(t)I(t) - \gamma_1 V(t) - \mu V(t), \\
\frac{dE}{dt} &= \beta S(t)I(t) + \beta_1 V(t)I(t) - \beta e^{-\mu\tau} S(t-\tau)I(t-\tau) - \beta_1 e^{-\mu\tau} V(t-\tau)I(t-\tau) - \mu E(t), \\
\frac{dI}{dt} &= \beta e^{-\mu\tau} S(t-\tau)I(t-\tau) + \beta_1 e^{-\mu\tau} V(t-\tau)I(t-\tau) - \gamma I(t) - \mu I(t) - \alpha I(t), \\
\frac{dR}{dt} &= \gamma_1 V(t) + \gamma I(t) - \mu R(t).
\end{aligned} \tag{29}$$

They analyzed the dynamic behavior of the model under pulse vaccination. Pulse vaccination is an effective strategy for the elimination of infectious disease. Using the discrete dynamical system determined by the stroboscopic map, they obtain an infection-free periodic solution. They also showed that the infection-free periodic solution is globally attractive when some parameters of the model under appropriate conditions. The permanence of the model was investigated analytically.

In [86], the authors proposed a fractional-order mathematical 5D dynamical system modelling an SVEIR model of infectious disease transmission in a chemostat is proposed. The model developed here has five components, S, V, E, I and R known as SVEIR model of infectious disease transmission in a chemostat. The population are classified as Susceptible individuals (S), Vaccinated individuals (V), Exposed individuals (E), Infected individuals (I), and Recovered individuals (R) and modelled by the following five-dimensional dynamical system of Fractional Differential Equations (FDEs) with the Caputo fractional derivative:

$$\begin{aligned}
{}_0^C D_t^\alpha S &= D(S_{in} - S) - (m_S + p)S - \mu(I)S, \\
{}_0^C D_t^\alpha V &= pS - (D + m_V)V - \theta\mu(I)V, \\
{}_0^C D_t^\alpha E &= \mu(I)(S + \theta V) - (D + m_E + \varepsilon)E, \\
{}_0^C D_t^\alpha I &= \varepsilon E - (D + m_I + \gamma)I, \\
{}_0^C D_t^\alpha R &= \gamma I - (D + m_R)R,
\end{aligned} \tag{30}$$

where p, θ, $1/\varepsilon$ and $1/\gamma$ are the vaccination rate, the vaccination factor reducing the risk of infection after vaccination, the average latency time spent in compartment E before moving to compartment I and the average duration elapsed in compartment I before recovery (R), respectively. m_S, m_V, m_E, m_I and m_R are the mortality rates of susceptible, vaccinated, exposed, infected and recovered individuals, respectively. μ represents the saturated incidence rate. A profound qualitative analysis was given and the analysis of the local and global stability of equilibrium points was carried out.

3.7. Mathematical modeling of HIV/AIDS epidemics (SIJA MODEL)

Human immunodeficiency virus (HIV), which leads to acquired immunodeficiency syndrome (AIDS), is a pandemic which is almost very dangerous and fatal if untreated and uncontrolled. Over 35 million people have died from AIDS-related illnesses since the start of the epidemic in 1981. Viral transmission typically occurs following exposure to cell-associated virus through: (1) contaminated blood products or syringes, (2) sexual intercourse and (3) mother to child in utero, during birth, or through breastfeeding. An individual may advance through several infective stages before developing full blown AIDS [87]. Virus number in the blood is a major indicator of the disease stages. Sometimes these stages are meant to correspond to CD4+ T-cell count ranges. In a normal healthy individual's peripheral blood, the level of CD4+ T-cells is between 800 and $1200/mm^3$ and once this number reaches 200 or below in an HIV infected patient, the person is classified as having AIDS. Without drug treatment, HIV-1 infection is nearly uniformly fatal within 5–10 years. With drug therapies, such as HAART (highly active antiretroviral therapy), treated individuals can live longer free of HIV-related symptoms [88].

Mathematical models have been used extensively in research into the epidemiology of HIV/AIDS to help improve our understanding of the major contributing factors to the pandemic. From the initial models of May and Anderson [89–91], various refinements have been added into modelling frameworks, and specific issues have been addressed by researchers [92–95]. The book [96] by Castillo-Chavez contains a review of HIV/AIDS modeling papers including single-group models, multiple-group models, and epidemiologic-demographic models. It also contains papers on AIDS models with HIV class age, variable infectivity, distributions for the AIDS incubation period, heterogeneity, and structured mixing.

To construct the model, the authors in [97] first divided the total population into a susceptible class of size S and an infectious class before the onset of AIDS and a full-blown AIDS group of size A which is removed from the active population. Based on the facts that the infectious period is very long ($\geq$ 10 years), the researchers further considered several stages of the infectious period. For simplicity, they only consider two stages according to clinic stages and papers [88,95] i.e., the asymptomatic phase (I) and the symptomatic phase (J). Thus, they first considered the following model [97]:

$$\begin{aligned} {}_0^{RL}D_t^{\alpha} S(t) &= \mu K - c\beta(1+bJ)S - \mu S, \\ {}_0^{RL}D_t^{\alpha} I(t) &= c\beta(1+bJ)S - (\mu + k_1)I + \gamma J, \\ {}_0^{RL}D_t^{\alpha} J(t) &= k_1 I - (\mu + k_2 + \gamma)J, \\ {}_0^{RL}D_t^{\alpha} A(t) &= k_2 J - (\mu + d)A, \end{aligned} \tag{31}$$

where, μK is the recruitment rate of the population, μ is the number of death rate constant. c is the average number of contacts of an individual per unit of time. β and $b\beta$ are probability of disease transmission per contact by an infective in the first stage and in the second stage, respectively. k_1 and k_2 are transfer rate constant from the asymptomatic phase I to the symptomatic phase J and from the symptomatic phase to the AIDS cases, respectively. γ is treatment rate from the symptomatic phase J to the asymptomatic phase I. d is the disease-related death rate of the AIDS cases.

In [98], Kheiri and Jafari presented a fractional order model of the transmission dynamics HIV/AIDS with random testing and contact tracing in Cuba, that is the generalization, to fractional order, of the model given by Mastroberardino et al. [99]:

$$\begin{aligned} {}_0^{C}D_t^{\alpha} S(t) &= \Lambda - (\varepsilon_1 u_1 \beta + (1-u_1)\beta)XS - \mu S, \\ {}_0^{C}D_t^{\alpha} X(t) &= (\varepsilon_1 u_1 \beta + (1-u_1)\beta)XS - \kappa XY - (\mu + \gamma + \kappa')X, \\ {}_0^{C}D_t^{\alpha} Y(t) &= \kappa XY + \kappa' - (\mu + (\varepsilon_2 u_2 \gamma + (1-u_2)\gamma))Y, \\ {}_0^{C}D_t^{\alpha} Z(t) &= \gamma X + (\varepsilon_2 u_2 \gamma + (1-u_2)\gamma)Y - \mu' Z, \end{aligned} \tag{32}$$

where $0 \leq \alpha \leq 1$. The model parameters are:

-Λ: constant recruitment rate of susceptible population;
-β : recruitment rate of new members of HIV-infected population infected by sexual transmission with X;
-γ: rate at which HIV-infected population develops AIDS;
-κ: rate at which undiagnosed HIV-infected population is diagnosed through contact tracing;
-κ': rate at which undiagnosed HIV-infected population is diagnosed through random testing;
-μ: mortality rate of the adult population;
-μ': mortality rate of the population with AIDS;
-u_1: the proportion of susceptible individuals that use condom;
-u_2: the proportion of diagnosed HIV-infected population that are under ART treatment;
-ε_1: efficacy of u_1;
-ε_2: efficacy of u_2.

The stability of the equilibria of the model are discussed using the stability theorem and using the fractional La-Salle invariance principle for fractional differential equations (FDEs). In this model, the susceptible population are transmitted to the undiagnosed HIV infected population by a mass action term. The undiagnosed HIV-infected population are infected by sexual transmission and move to the diagnosed class in two ways: one is through a mass action term that represents contact tracing, and the other is through a linear term that represents random or voluntary testing. In addition, it is assumed that the diagnosed HIV-infected population and the AIDS people can not transmit the infection due to the Cuban health care system [99]. It is worth noting that 99% of the infection is done in Cuba via sexual contact [100], so infection by nonsexual transmission is neglected.

Kheiri and Jafarin [98] presented a general formulation for a FOCP, in which the state and co-state equations are given in terms of the left fractional derivatives. This approach simplifies the use of fractional numerical methods to solve the state and co-state equations. For numerical simulation of the FOCP, they developed the Forward-Backward sweep method (FBSM) using the Adams-type predictor-corrector method. They considered the control parameters of the model as time dependent controls and formulate an optimal control problem. Conditions for fractional optimal control of the disease are derived and analyzed. The state and co-state equations were characterized by left fractional derivatives and the numerical method is used to numerically compute the solutions of the optimality system. Also, the efficacy of the fractional derivative order α ($0.6 \leq \alpha \leq 1$) on the HIV/AIDS epidemic model and the controls was investigated.

3.8. Mathematical modeling of smoking epidemics (POSQL MODEL)

Smoking is the major problem in the entire world effecting healthy community. Smoking effects different organs of human body caused more than one million deaths in the world. A chance of heart attack in smoker is 70% more as compared to nonsmoker. Similarly, the incident rate of lung cancer of smoker is 10% more than nonsmoker. The main effects of short term smoking are coughing, stained teeth, high blood pressure and bad breath. The major effects of long term smoking are gum disease, stomach ulcer, lung cancer, heart disease, throat cancer and mouth cancer in the recent years. The life of

smoker is also 12–13 years shorter than non-smoker. According to the reports of world health organization (WHO) smoking kills many individual in the entire world. Every scientist, doctor and mathematician tries to control the effect of smoking. The lot of smoking models are presented by the researchers. Erturk et al. examined the smoking model related with Caputo fractional derivative [101]. Zaman studied the optimal control of the smoking models and present the qualitative analysis of dynamics of smoking [102,103]. Analysis of cigarette smoking and lung cancer is presented in [104]. Garsow et al. [105] described the mathematical analysis of tobacco use their decline. Some more interesting studies about dynamics of smoking is discussed in [106–109].

The concept of mathematical modeling has been prolonged to define the stability and qualitative features of giving up smoking models from 2000. Smoking model is divided into five subdepartment like potential smoker $P(t)$, the occasional smoker $O(t)$, smoker $S(t)$, temporarily quit smoker $Q(t)$ and permanently quit smoker $L(t)$. The proposed smoking model in the form of system of nonlinear differential equation is given by [110]:

$$\begin{aligned}
\frac{dP}{dt} &= \Lambda - \beta PS - \mu P,\\
\frac{dO}{dt} &= \beta PS - \alpha_1 O - \mu O,\\
\frac{dS}{dt} &= \alpha_1 O + \alpha_2 SQ - (\mu + \gamma)S,\\
\frac{dQ}{dt} &= -\alpha_2 SQ - \mu Q + \gamma(1-\delta)S,\\
\frac{dL}{dt} &= \delta\gamma S - \mu L.
\end{aligned} \tag{33}$$

In this model, Λ is represent the recruitment rate in P, β is the effective contact rate between S and P, μ is the natural death rate, α_1 is the rate at which occasional smokers become regular smokers, α_2 and γ represents the contact rate between smokers and temporary quitters who revert back to smoking and the rate of quitting smoking respectively, $(1-\delta)$ is the fraction of smokers who temporary quit smoking (at the rate γ), δ is the remaining fraction of smoking which represents permanently quit smoking.

The fractional smoking model in the sense of Caputo fractional derivatives could be described as follows [110]:

$$\begin{aligned}
{}_0^C D_t^{\phi_1} P(t) &= \Lambda - \beta PS - \mu P,\\
{}_0^C D_t^{\phi_2} O(t) &= \beta PS - \alpha_1 O - \mu O,\\
{}_0^C D_t^{\phi_3} S(t) &= \alpha_1 O + \alpha_2 SQ - (\mu + \gamma)S,\\
{}_0^C D_t^{\phi_4} Q(t) &= -\alpha_2 SQ - \mu Q + \gamma(1-\delta)S,\\
{}_0^C D_t^{\phi_5} L(t) &= \delta\gamma S - \mu L.
\end{aligned} \tag{34}$$

In this study smoking epidemic model has been investigated as follows:

(i) Laplace Adomian decomposition method for mathematical models based on system of fractional order differential equations is more powerful approach to compute the convergent solutions.
(ii) The convergence analysis is also provided to demonstrate the efficiency of the method.
(iii) The constructed series by Laplace Adomian decomposition method for smoking model show a good agreement to control the bad impact of smoking for different time period and to eradicate a death killer factor in the world.
(iv) Introduced the stability analysis theory and sensitivity analysis of mathematical epidemic models in the nonlinear system which represent both the local and global behavior of smoking dynamics.
(v) Estimated the parameter that characterize the behavior of disease and present numerical simulations.

The pivotal aim of the resent work is to obtain an approximated analytical solution for the fractional smoking epidemic model with the aid of a novel technique called q-homotopy analysis transform method (q-HATM) [111]. The considered nonlinear mathematical model has been effectively employed to elucidate the evolution of smoking in a population and its impact on public health in a community. The researchers found some new approximate solutions in a series form, which converges rapidly, and the proposed algorithm provides auxiliary parameters, which are very reliable and feasible in controlling the convergence of obtained approximate solutions. Further, they presented novel simulations for all cases of results to validate the applicability and effectiveness of proposed scheme. The outcomes of the study reveal that the q-HATM is computationally very effective to analyse nonlinear fractional differential equations arises in daily life problems.

3.9. Mathematical modeling of shigellosis and norovirus outbreak (SEIAR MODEL)

Shigellosis (bacillary dysentery), the result of infection with Shigella, is an enteric infectious disease responsible for approximately 1,100,000 deaths per year worldwide [112]. As approximately two-thirds of those who die from shigellosis are children under 5 years of age, it is one of the most common diarrhea-related causes of morbidity and mortality in children in

developing countries [113]. Shigellosis epidemics usually occur in areas with crowding and poor sanitary conditions, where person-to-person transmission or contamination of food or water by the organism is common [114–119]. In China, many private wells supplying water to schools are built in close proximity to sources of pollution, including toilets, septic tanks, sewer ditches, and lakes and ponds into which sewage is discharged. As water from these wells is often not treated before being piped into schools, waterborne outbreaks of Shigella frequently occur [117], with devastating effects on students, their families, and schools.

Many outbreak control strategies developed by primary-level health departments in China are empirically-driven. This can be attributed to a lack of data regarding the rate of morbidity in the absence of intervention, making it difficult to estimate whether the efficacy of a single or combined intervention could be decreased if implemented using traditional methods. In these circumstances, researchers often perform mathematical modeling to estimate the total attack rate (TAR), an indicator of the extent of an outbreak [120–124]. A bacillary dysentery model with seasonal fluctuation was formulated and studied by Bai et al. [125].

Fortunately, a waterborne pathogen model termed the Susceptible-Infectious-Recovered-Water (SIRW) model can be used to examine disease outbreaks that occur via multiple transmission pathways [126], such as shigellosis. The SIRW model is a simple ordinary differential equation model that extends the classic SIR framework by adding a compartment (W) that tracks the pathogen concentration in water. Infected individuals shed the pathogen into water compartments, and new infections arise both through exposure to contaminated water as well as by the classic SIR person-person transmission pathway. The researchers developed a SEIARW model to examine the efficacy of different intervention strategies in controlling an outbreak of shigellosis at a primary school in Changsha City, China.

In [127], the authors gave the development of the SEIARW model, where individuals were characterized according to their epidemiological status as susceptible (S), exposed (E, infected but not yet fully contagious), infectious (I), asymptomatic (A), and recovered (R); W denotes the reservoir (water) compartment. The susceptible individuals become infected (i.e., move from S to E) by contact with either infected/asymptomatic individuals or contaminated water at rates of βSI, βkSA and $\beta_W SW$ respectively, where β and β_W are the probability of transmission per contact, k is the relative transmissibility of asymptomatic to symptomatic individuals. As exposed individuals become infectious after an incubation period, they move from E to I at a rate of $(1-p)\omega E$ and E to A at a rate of $p\omega E$, where $1/\omega$ is the incubation period of the disease and p is the proportion of asymptomatic individuals. After the infectious period has passed, infectious and asymptomatic individuals may move to R at a rate of γI and $\gamma' A$ respectively, where $1/\gamma$ and $1/\gamma'$ are the infectious period of the I and A. Infectious and asymptomatic individuals can in turn contaminate the water compartment by shedding the pathogen into W at a shedding rate of μI and $\mu' A$, where μ and μ' are the shedding coefficients. The pathogen in W will subsequently leave the water compartment at a rate of εW, where $1/\varepsilon$ is the lifetime of the pathogen. The corresponding model equations are as follows:

$$\begin{aligned}
\frac{dS}{dt} &= -\beta S(I+kA) - \beta_W SW,\\
\frac{dE}{dt} &= \beta S(I+kA) + \beta_W SW - \omega E,\\
\frac{dI}{dt} &= (1-p)\omega E - \gamma I,\\
\frac{dA}{dt} &= p\omega E - \gamma' A,\\
\frac{dR}{dt} &= \gamma I + \gamma' A,\\
\frac{dW}{dt} &= \mu I + \mu' A - \varepsilon W.
\end{aligned} \tag{35}$$

A disease with similar epidemic models above called Norovirus which is one of the most important pathogens of infectious diarrhea and outbreaks of all ages [128–130]. In the United States, Norovirus causes approximately 21 million cases each year [129], 71,000 hospitalizations [131], and 800 deaths [129,132]. In developing countries, there are frequent outbreaks of medical institutions and schools [133], which have a great impact on the health of residents. The disease is mainly transmitted through the fecal-oral route, and the infection dose is very low. Ingestion of 18 viruses at a time can cause infection [134]. Therefore, it is easy to cause transmission, usually by human contact, and water or Food spread. School outbreaks can also lead to absenteeism or even suspension of classes, affecting normal teaching order and increasing the burden of family care for children. Therefore, in-depth study of the dynamic characteristics of Norovirus infectious diarrhea outbreaks, and the evaluation of the effects of various types of prevention and control measures have important public health significance.

Based on the natural history of Norovirus-infected diarrhea, the researchers established the integer order SEIAR model of Norovirus transmission in schools. Taking an outbreak event in a city in 2007 as an example, the dynamic characteristics of Norovirus were studied and the key prevention and control was quantitatively evaluated. But the results which demonstrated the effect of match could be improved further to reflect the spread of Norovirus, especially the transmission speed before the intervention.

The SEIAR model is the most common method for studying the dynamic characteristics of some infectious disease, such as Norovirus, influenza, worm propagation The classical model of the SEIAR model considers that the total human population N is divided into five subpopulations: $S(t)$ susceptible humans, $E(t)$ exposed humans (infected but not yet fully contagious), $I(t)$ infected humans, $A(t)$ asymptomatic humans, $R(t)$ recovered (or removed) humans. Hence, the classical model consists of five ordinary differential equations for the five independent functions of the form [135]:

$$\begin{aligned}
\frac{dS}{dt} &= -\beta S(I+\kappa A),\\
\frac{dE}{dt} &= \beta S(I+\kappa A) - \mu\omega' E - (1-\mu)\omega E,\\
\frac{dI}{dt} &= (1-\mu)\omega E - \gamma I,\\
\frac{dA}{dt} &= \mu\omega' E - \gamma' A,\\
\frac{dR}{dt} &= \gamma I + \gamma' A.
\end{aligned} \tag{36}$$

Based on the integer order SEIAR model, we propose the following fractional SEIAR model using the Caputo fractional derivative with order α_i $(i = 1, 2, \cdots, 5)$:

$$\begin{aligned}
\lambda_{\alpha_1}\, {}_0^C D_t^{\alpha_1} S &= -\beta S(I+\kappa A),\\
\lambda_{\alpha_2}\, {}_0^C D_t^{\alpha_2} E &= \beta S(I+\kappa A) - \mu\omega' E - (1-\mu)\omega E,\\
\lambda_{\alpha_3}\, {}_0^C D_t^{\alpha_3} I &= (1-\mu)\omega E - \gamma I,\\
\lambda_{\alpha_4}\, {}_0^C D_t^{\alpha_4} A &= \mu\omega' E - \gamma' A,\\
\lambda_{\alpha_5}\, {}_0^C D_t^{\alpha_5} R &= \gamma I + \gamma' A,
\end{aligned} \tag{37}$$

where some new parameters λ_{α_i} $(i = 1, 2, \cdots, 5)$ are introduced, which have dimension of $(days)^{\alpha_i - 1}$ on the left sides of the equations to preserve units. This ensures that both sides of the equations have the same dimension $(days)^{-1}$.

In this paper, we will use the single-term and multi-term fractional order SEIAR model to describe the outbreak of norovirus with the fractional derivatives in the sense of Caputo in sections 6 and 7. These fractional SEIAR models have different values of fractional order. In order to obtain the numerical solution of the fractional equations, the GMMP scheme is used as an implicit difference scheme. The Newton method is used to solve this implicit difference scheme which can be considered as a nonlinear equations. Furthermore, the corresponding inverse problem of parameter estimation is investigated by the modified hybrid Nelder-Mead simplex search and particle swarm optimization algorithm [136]. Using the statistics from the norovirus outbreak in a middle school in China in 2007 [135], the parameters of the single-term and multi-term fractional order SEIAR model can be determined, respectively, and both the numerical results of two fractional order SEIAR models are in good agreement with the real data details in sections 6 and 7.

4. Numerical methods for the fractional order differential equation

There are various numerical methods which have been applied to solve the fractional order equations, including the Power Series Method [27], the Predictor Corrector Method [27,29], the Mellin Transform Method [137], and others. In this paper, we applied the GMMP scheme (Gorenflo-Mainardi-Moretti-Paradisi) [81] and Newton method to solve the equations mentioned above, which is much more efficient than other numerical methods. For the sake of simplicity, we consider the equations as form:

$$\lambda \odot {}_a^C D_t^{\alpha} x(t) = f(t, x(t)) \tag{38}$$

where $x(t) = (S(t), E(t), I(t), A(t), R(t))^T$, $\lambda = (\lambda_{\alpha_1}, \lambda_{\alpha_2}, \lambda_{\alpha_3}, \lambda_{\alpha_4}, \lambda_{\alpha_5})^T$ and ${}_a^C D_t^{\alpha}$ denotes the Caputo fractional derivative. In order to obtain the numerical solution of the fractional differential equations, we discrete in time using the uniform grids with $0 < \alpha < 1$, that is $t_j = a + jh$, $j = 0, 1, 2, \cdots, N$, $Nh = t - a$. As we know, the Riemann-Liouville and Grünwald-Letnikov fractional derivatives can be approximated using the following formula,

$${}_a^{RL} D_t^{\alpha} x(t) = {}_a^{GL} D_t^{\alpha} x(t) = \lim_{h\to 0} \frac{1}{h^{\alpha}} \sum_{k=0}^{N} c_k^{\alpha} x(t_{N-k}) \approx \frac{1}{h^{\alpha}} \sum_{k=0}^{N} c_k^{\alpha} x(t_{N-k}), \tag{39}$$

and the Caputo fractional derivatives can be approximated by the following relation

$${}_a^C D_t^{\alpha} x(t) \approx \frac{1}{h^{\alpha}} \sum_{k=0}^{N} c_k^{\alpha} \left[x(t_{N-k}) - \sum_{j=0}^{n-1} \frac{(t-a)^j x^{(j)}(a)}{j!} \right], \tag{40}$$

where $c_k^{\alpha} = (-1)^k \binom{\alpha}{j}$ are binomial coefficients.

This method was first introduced by Gorenflo in [81] and is known as the GMMP scheme in [138]. Based on the GMMP scheme, we can present the numerical techniques for simulating fractional order differential equations. In order to explain this method, the fractional order nonlinear Eq. (37) can be written as:

$$\begin{aligned} \lambda \odot {}_a^C D_t^\alpha x(t) &= f(t, x(t)), 0 \le t \le T, \\ x^{(k)}(a) &= x_0^{(k)}, k = 0, 1, \cdots, n-1. \end{aligned} \tag{41}$$

It follows from formula (40) that

$$\lambda \odot \sum_{k=0}^{N} c_k^\alpha \left[x(t_{N-k}) - \sum_{j=0}^{n-1} \frac{(t-a)^j x^{(j)}(a)}{j!} \right] = h^\alpha f(t_N, x(t_N)), \tag{42}$$

i.e,

$$x(t_N) = h^\alpha \oslash \lambda \odot f(t_N, x(t_N)) + \sum_{j=0}^{n-1} \frac{(t-a)^j x^{(j)}(a)}{j!} - \sum_{k=1}^{N} c_k^\alpha \left[x(t_{N-k}) - \sum_{j=0}^{n-1} \frac{(t-a)^j x^{(j)}(a)}{j!} \right]. \tag{43}$$

In particular, if $0 < \alpha \le 1$, the above formula (43) can be written as follows:

$$x(t_N) = h^\alpha \oslash \lambda \odot f(t_N, x(t_N)) + x(a) - \sum_{k=1}^{N} c_k^\alpha [x(t_{N-k}) - x(a)]. \tag{44}$$

Based on the Grünwald-Letnikov formula, we can present an implicit difference scheme (44) which can be considered as an equation with respect to an unknown variable $x(t_N)$. Then, we can use the Newton method to solve the value of $x(t_N)$ by the Eq. (44).

The Newton method is an effective method of solving nonlinear equations. For the nonlinear equations $F(x) = 0$, the Newton method is expressed as:

$$x_{n+1} = x_n - J_F(x_n)^{-1} F(x_n), n = 0, 1, 2, \cdots, \tag{45}$$

where $J_F(x_n)$ is the Jacobian matrix at x_n. The LU factorization of $J_F(x_n)$ can be used to solve the above equations for definiteness in the description of Newton algorithm, and any other appropriate factorization such as QR or Cholesky can be used as well. The inputs of the algorithm are the initial iterate x_0, the nonlinear map F, and a termination tolerances ε. The details of the Newton algorithm are:

Step i: Compute and factor the Jacobian matrix $J_F(x_0) = LU$,
Step ii: Solve the linear equation $LUs = -F(x_0)$, $x = s + x_0$,
Step iii: While the x satisfies the condition $\|x - x_0\| > \varepsilon$, then
(iii.a) Let $x_0 = x$, then factor the Jacobian matrix $J_F(x_0) = LU$,
(iii.b) Solve the linear equation $LUs = -F(x_0)$, $x = s + x_0$,
(iii.c) Compute and evaluate $\|x - x_0\|$. If $\|x - x_0\| > \varepsilon$, goto step (iii.a).

Then we can get the output $x = x(t_N)$, i.e., the solution of the Eq. (44). In this paper, we use the GMMP scheme and Newton method to obtain the numerical solution of the fractional systems.

5. The technique for parameter estimation in fractional order non-linear systems

An exploration using a model reflecting the behaviour of a real system is known as the forward problem, whereas the process of fitting model parameters to a measurement or measurements is known as the inverse problem. It is difficult to estimate parameters of fractional order nonlinear model. This problem will become more difficult when the range of the parameters is large and the function f is highly non-linear with respect to the unknown parameters in the fractional nonlinear model. To improve the fitting process and its robustness and avoid being trapped in a local minimum, strict procedures can be followed, which involve narrowing the search space. Therefore, the search for a global minimum has been formulated as a constrained optimisation problem. To analyse the reliability of our model in a quantitatively correct way, parameters need to be globally determined.

In this section, a feasible and reliable parameter estimation technique is presented for the purpose of obtaining the global minimum to the optimisation problem. A technique is proposed for estimating parameters in a fractional order nonlinear model. The fractional order nonlinear system (41) can be written as a model with m unknown parameters:

$$\begin{aligned} \lambda \odot {}_a^C D_t^\alpha x(t) &= f(t, x(t), P), 0 \le t \le T, \\ x^{(k)}(a) &= x_0^{(k)}, k = 0, 1, \cdots, n-1, \end{aligned} \tag{46}$$

where $x = (x_1, x_2, x_3, x_4, x_5)^T$ are state variables and $f = (f_1, f_2, \cdots, f_n)^T$ are n-dimensional vector functions, and every $f_i (i = 1, 2, \cdots, n)$ may be nonlinear with respect to the unknown parameters $P = (p_1, p_2, \cdots, p_m)^T$, m is the number of parameters.

In the following, we will introduce the method of parameter estimation with a modified hybrid Nelder-Mead simplex search and particle swarm optimization [136]. Both the hybrid Nelder-Mead simplex search (NMSS) ([139]) and the particle swarm optimisation (PSO) ([140]) have been widely used in solving challenging optimisation problems which are widely used for identifying parameter. However, the literature shows that the practical use of NMSS and PSO are both limited, since NMSS is likely to be trapped in a local optima and PSO has a slow convergence rate. Interestingly, the combined use of NMSS and PSO has been demonstrated to be outperform both NMSS and PSO in terms of solution quality and convergence rate.

In the NMSS-PSO parameter estimation process, the role assigned to NMSS and PSO is different due to their different functionalities. The NMSS focuses on exploitation and PSO focuses on exploration. The combination of the two methods makes full use of the merits of each method. Specifically, NMSS is used to exploit the current solution space and PSO focuses on the exploration of the unknown space. The obvious distinctions between NMSS and PSO mainly exist in their choice of initial points and the manner with which they proceed towards the solution: NMSS uses predetermined initial points and moves towards points with better objective function values, while PSO uses a set of random initial points and through iterations moves away from points with worse objective function values. The PSO proceeds by moving towards those points which have better function values, while the NMSS evolves by moving away from a point which has the worst performance. The modified hybrid Nelder-Mead simplex search and particle swarm optimization (MH-NMSS-PSO) method has been used to estimate parameters for integer and fractional model, which takes the best advantages of both the NMSS method and the PSO method. In the following, we will use the MH-NMSS-PSO method to conduct the parameter estimation for fractional order nonlinear models. Taking the better characteristics of each method, we propose the MH-NMSS-PSO method as follows.

Suppose that $P = (p_1, p_2, \cdots, p_m)^T \in \Omega$, where $\Omega = [p_1^{(min)}, p_1^{(max)}] \times [p_2^{(min)}, p_2^{(max)}] \times \cdots \times [p_m^{(min)}, p_m^{(max)}]$ is a bounded domain.

Let $x(t_j)$ be one of numerical solutions of Eq. (46) with the given parameters $P = (p_1, p_2, \cdots, p_m) \in \Omega$ which is obtained by the GMMP scheme and Newton method, the approximation of the unknown parameter vector $P^* = (p_1^*, p_2^*, \cdots, p_2^*)$ is determined by the root-mean-square error (rMSE)

$$g(P^*) = \min_{P\in\Omega} g(P) = \min_{p\in\Omega} \sqrt{\frac{\sum_{j=0}^{N} \left(x(t_j) - x_j\right)^2}{N+1}}, \tag{47}$$

where x_j are real data.

The MH-NMSS-PSO method tries to find a potential global minimum $g(P^*)$ in the equation with the parameters $P \in \Omega$. The MH-NMSS-PSO method takes the advantages of both the NMSS method and the PSO method to conduct the inverse problem. It starts with $(3m+1)$ initial particles, which is constructed in two parts. Firstly, the predetermined points is employed to form an initial simplex of $(m+1)$ particles which is used in the NMSS method, and the $2m$ paticles are randomly generated in the PSO method. Then, we sotred the total $(3m+1)$ particles from smallest to largest by the function values $g(P)$ in Eq. (47). In the following, the best $(m+1)$ particles are handled by the NMDD method, while the last $2m$ particles are adjusted by the PSO method. Then the algorithm for the MH-NMSS-PSO method is summarised as follows:

Step 1: Initialization. Generate a population of size $3m+1$.

For the minimization of the functions $g(P)$ of m variables (unknown parameters), create $(m+1)$ vertex points $P_i = (p_{1,i}, p_{2,i}, \cdots, p_{m,i}) \in \Omega, (i = 1, 2, \cdots, m+1)$ to form an initial m-dimensional simplex. Evaluate the function value at each extreme point (or vertex) of the simplex, i.e. $m+1$ particles are constructed via the standard starting point used in the NMSS, and a step size of $(p_j^{(max)} - p_j^{(min)})/(m+1)$ at each coordinate direction to form an initial simplex for the NMSS part, i.e. $p_{j,i} = p_j^{(min)} + (i-1) \times (p_j^{(max)} - p_j^{(min)})/(m+1), \ (j = 1, 2, \cdots, m; i = 1, \cdots, m+1)$. $2m$ particles are randomly generated in each dimension for the PSO part, $P_i = (p_{1,i}, p_{2,i}, \cdots, p_{m,i}) \in \Omega, \ (i = m+2, \cdots, 3m+1)$, where $p_{j,i} = p_j^{(min)} + Rand \times (p_j^{(max)} - p_j^{(min)})(j = 1, 2, \cdots, m; i = m+2, \cdots, 3m+1)$ and Rand is a random number in the range (0,1). Moreover, the particle's initial velocities in each dimension are selected by the following:

$$V_{j,i} = (V_j^{(max)} - V_i^{(min)})/L_j (j = 1, 2, \cdots, m; i = m+2, \cdots, 3m+1), \tag{48}$$

where $L_j (j = 1, 2, \cdots, m)$ are selected integers.

Step 2: Evaluation and ranking: evaluate the objective function value $g(P)$ of each particle. Rank them based on the objective function value;

$$g(p_1) \le g(p_2) \le \cdots \le g(p_{3m+1}). \tag{49}$$

Step 3: NMSS method: apply the NMSS method to the best $m+1$ particles and replace the $(m+1)$th particle with the update as follows:

(3.1) Calculate P_0, the center of gravity of all points except P_{m+1}, i.e. $P_0 = (p_{1,0}, p_{2,0}, \cdots, p_{m,0}) \in \Omega$, where $p_{j,0} = \frac{\sum_{i=1}^{m} p_{j,i}}{m} (j = 1, 2, \cdots, m)$.

(3.2) Reflection: In each iteration, determine P_{m+1}, P_m and P_1 vertices, indicating the highest, the second highest and the lowest function values that occur, respectively. Let $g(P_{m+1})$, $g(P_m)$ and $g(P_1)$ represent the corresponding observed function values. Compute the reflected point

$$P_r = (1+\kappa)P_0 - \kappa P_{m+1}, \tag{50}$$

where κ is the reflection coefficient ($\kappa > 0$) using the suggested value $\kappa = 1$ [139]. $P_r = (p_{1,r}, p_{2,r}, \cdots, p_{m,r}) \in \Omega$, $p_{j,r} = (1+\kappa)p_{j,0} - \kappa p_{j,m+1} (j = 1, 2, \cdots, m)$. If $g(P_1) \le g(P_r) \le g(P_m)$, then P_r replaces P_{m+1}, else go to step (3.3).

(3.3) Expansion: If $g(P_r) \le g(P_1)$, then compute the expanded point

$$P_e = \gamma P_r + (1-\gamma)P_0, \tag{51}$$

where γ is the expansion coefficient using the suggested value $\gamma = 2$ [139]. $P_e = (p_{1,e}, p_{2,e}, \cdots, p_{m,e})$, $p_{j,e} = \gamma p_{j,r} + (1-\gamma)p_{j,0} (j = 1, 2, \ldots, m)$. If $g(P_e) \le g(P_1)$, then P_e replaces P_{m+1}, otherwise P_r replaces P_{m+1}. Else continue at step (3.4).

(3.4) Contraction: if $g(P_r) > g(P_m)$, then if $g(P_r) \le g(P_{m+1})$, then P_r replaces P_{m+1}, compute the contracted point

$$P_c = \beta P_{m+1} + (1-\beta)P_0. \tag{52}$$

where $\beta (0 < \beta < 1)$ is the expansion coefficient using the suggested value $\beta = 0.5$ [139]. $P_c = (p_{1,c}, p_{2,c}, \cdots, p_{m,c})$, $p_{j,c} = \beta p_{j,m+1} + (1-\beta)p_{j,c} (j = 1, 2, \cdots, m)$. If $g(P_c) \le g(P_{m+1})$, then P_c replaces P_{m+1}. Else go to step (3.5).

(3.5) Shrink: For all but the best point, replace the point with

$$P_i = \sigma P_i + (1-\sigma)P_1, \tag{53}$$

where σ is the shrinkage coefficient with the suggested value $\sigma = 0.5$ and P_i denotes the vertex point for $i = 2, 3, \cdots, m+1$.

Step 4: Particle swarm optimization: apply the PSO operator for updating the last $2m$ particles with the worst objective function value as follows:

(4.1) Velocity and position update. Assign the best positions $Pb_i = P_i (i = m+2, \cdots, 3m)$ (initialize randomly all particles positions in step 1 and the global best location $P_g = P_{m+2}$. The particles velocity and position are updated by the following equations:

$$V_{j,i}^{new} = \omega \times V_{j,i}^{old} + C_1 \times Rand_1 \times (Pb_{j,i} - P_{j,i}^{old}) + C_2 \times Rand_2 \times (P_{g_j} - P_{j,i}^{old}),$$
$$P_{j,i}^{new} = P_{j,i}^{old} + V_{j,i}^{new}, j = 1, 2, \cdots, m; i = m+2, \cdots, 3m+1,$$

where C_1 and C_2 are two pre-determined positive constants, ω is an inertia weight and $Rand_1$ and $Rand_2$ are random numbers in the range $(0, 1)$. Considering the ranges of the search space in different dimensions, we use $C_1 = 0.8, C_2 = 0.3$ and $\omega = [0.5 + (Rand/2.0)]$ in our case.

(4.2) Imposed boundaries. The absorbing walls are imposed to drive particles to the pre-determined parameter domains [141]. Thus, it avoids physically impossible solutions by assuming the velocity in a certain dimension is zero when a particle hits the boundary placed on that parameter.

(4.3) PSO iteration. Return to step 4 and start a new PSO iteration until it reaches the largest PSO iteration time S_{iter}.

Step 5: Evaluate and rank again for all $3m+1$ particles. Discriminate the stopping criterion: if $S_c < \varepsilon$, where ε is a small error parameter, the loop will stop. The criterion is defined by

$$S_c = \sqrt{\sum_{i=1}^{m+1} \frac{(\bar{g} - \sqrt{g_i})^2}{m+1}} \tag{54}$$

where $\bar{g} = \sum_{i=1}^{m+1} \frac{g_i^*}{m+1}$ and $g_i^* = \sqrt{g_i} = \sqrt{g_i(p_1, p_2, \cdots, p_m)}$. The algorithm will stop when either (54) is satisfied or the number of iterations reaches the maximum iteration count.

Step 6: Output the best estimated parameter values $P = (p_1, p_2, \cdots, p_m)$.

This parameter estimation technique can be implemented in a straightforward manner for the purpose of solving inverse problems governed by fractional linear or nonlinear dynamics, since it does not require gradient computation and is therefore derivative free. The NMSS-PSO algorithm has been outlined in detail in [136].

6. Application to parameter estimation in the fractional SEIAR model

In this section, the MH-NMSS-PSO scheme is employed to estimate the fractional orders and parameters for the fractional-order Norovirus infection system in Section 3.9. The results can verify the efficiency of both the GMMP scheme presented in Section 4 and the MH-NMSS-PSO presented in Section 5 for the inverse problem.

In the reference [135], they used the data about a Norovirus infectious diarrhea incident reported in a school in China. The information includes the number of people affected, the onset time of all cases, the intervening time of the department of the centers for disease control and prevention, the preventive and control measures, etc. The details of the outbreak are as follows: the department of the centers for disease control and prevention of a city received a telephone report from a middle school on March 8, saying that there were more than ten cases of vomiting, abdominal pain and diarrhea in the school recently. The following case definitions were established: vomiting or diarrhea and other symptoms such as abdominal pain, fever, headache and dizziness have occurred among the students and staff of the school since March 5. There are 93 classes in 5 grades in the school, with 5225 students and 430 teachers. The number of cases reached a peak on 8 March. After the intervention on 8 March, isolation measures were taken. The epidemic situation began to decline gradually. The authors used the integer order SEIAR model to predict the number of the infected people with the selected values of the parameters: $\beta = 8.3452 \times 10^{-4}$, $\kappa = 3.9065 \times 10^{-11}$, $\omega = 1$, $\omega' = 1$, $\mu = 0.3$, $\gamma = 0.3333$ and $\gamma' = 0.03846$,

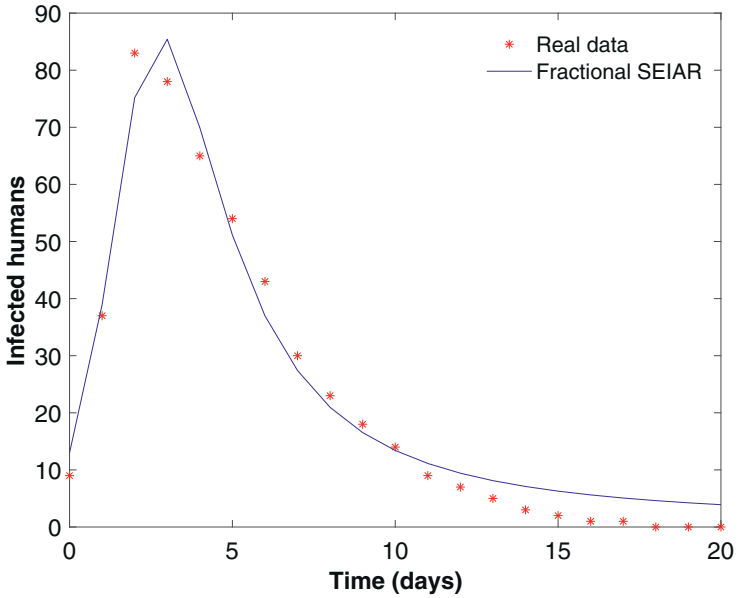

Fig. 1. Number of infected humans $I(t)$ in a middle school in the 2007: Comparison of numerical results of one-term fractional SEIAR model with the real data with the estimated parameters obtained by MH-NMSS-PSO method. The root-mean-square error is rMSE = 4.0792.

and the root-mean square error between the numerical solutions of integer order SEIAR model with the real data is rMSE = 7.9138 [135].

In this paper, we use the modified hybrid Nelder-Mead simplex search and particle swarm optimization (MH-NMSS-PSO) algorithm to estimate the parameters of fractional SEIAR model (37) to the real data. The real data of a 2007 Norovirus outbreak in a middle school is used as the known data to perform the inverse problem of parameter estimation. The parameters $\lambda_{\alpha_i}(i = 1, 2, \cdots, 5)$ are used to ensure that both sides of the equation have the same dimension, and these constants can be divided throughout and combined with the parameters on the right-hand side. There are five fractional order parameters and totally seventeen parameters that should be estimated. In this inverse procedure, the unknown parameters vector is taken as $P = (\lambda_1, \cdots, \lambda_5, \alpha_1, \cdots, \alpha_5, \beta, \mu, \kappa, \omega, \omega', \gamma, \gamma')$. Each of the parameters in the fractional order SEIAR model (37) has its particular biological meaning and each parameter has a corresponding value range. Therefore, based on these ranges, we select some appropriate intervals and initial velocities as follows:

$$
\begin{array}{ll}
0 \le \lambda_i = p_i \le 2, i = 1, 2, \cdots, 5, & 0 \le \alpha_j = p_{j+5} \le 1, j = 1, 2, \cdots, 5 \\
1 \times 10^{-4} \le \beta = p_{11} \le 1 \times 10^{-3}, & 1 \times 10^{-11} \le \kappa = p_{12} \le 1 \times 10^{-10} \\
0.01 \le \mu = p_{13} \le 0.3, & 1 \le \omega = p_{14} \le 2 \\
1 \le \omega' = p_{15} \le 2, & 0.3 \le \gamma = p_{16} \le 1 \\
0.05 \le \gamma' = p_{17} \le 0.09 &
\end{array}
$$

and

$$
V_i = \begin{cases}
0.02 & , \quad i = 1, 2, \cdots, 5; \\
0.01 & , \quad i = 6, 7, \cdots, 10; \\
1 \times 10^{-4} & , \quad i = 11; \\
1 \times 10^{-11} & , \quad i = 12; \\
0.01 & , \quad i = 13; \\
0.025 & , \quad i = 14, 15; \\
0.01 & , \quad i = 16, 17.
\end{cases}
$$

Using the same initial values and the time as $t = 20$ days, we apply the MH-NMSS-PSO to estimate model parameters from the real data based on the numerical solution solved by the GMMP scheme. Fig. 1 shows the comparison of numerical results of fractional SEIAR model with the real data and the calculated model parameters P^* are:

$$
\begin{array}{lllll}
\lambda_1 = 0.6182, & \lambda_2 = 0.8757, & \lambda_3 = 0.1106, & \lambda_4 = 0.9341, & \lambda_5 = 0.4627, \\
\alpha_1 = 0.9049, & \alpha_2 = 0.6940, & \alpha_3 = 0.7945, & \alpha_4 = 0.6637, & \alpha_5 = 0.8279, \\
\beta = 1 \times 10^{-3}, & \kappa = 5.6636 \times 10^{-11}, & \mu = 0.0382, & \omega = 1.0038, & \omega' = 1.0000, \\
\gamma = 0.3458, & \gamma' = 0.0737. & & &
\end{array}
$$

As can be seen from Fig. 1 that, the root-mean square error between the numerical solutions of fractional SEIAR model and the real data is rMSE = 4.0792, which suggests that both the GMMP scheme and the MH-NMSS-PSO method are valid in

dealing with inverse problems for the fractional SEIAR system, and the fractional SEIAR model provides better fit to the real data than the interger order SEIAR model.

7. Application to parameter estimation in the multi-term fractional SEIAR model

7.1. Multi-term fractional order SEIAR model of norovirus outbreak

As we known, the multi-term fractional order differential equation have played an important role in capturing the behaviour of real materials, especially in the field of the viscoelastic mechanics. In the recent years, some studies has shown that the multi-term fractional differential equation can also provide a better epidemic model than integer order derivative [10]. For searching a better norovirus epidemic system which is capable of providing numerical results that agree much better with the real data, we propose the following multi-term fractional order SEIAR model:

$$\begin{aligned}
{}_0^C D_t^{\xi_1,\cdots,\xi_r,\xi_0} S(t) &= -\beta S(I+\kappa A),\\
{}_0^C D_t^{\theta_1,\cdots,\theta_r,\theta_0} E(t) &= \beta S(I+\kappa A) - \mu\omega' E - (1-\mu)\omega E,\\
{}_0^C D_t^{\phi_1,\cdots,\phi_r,\phi_0} I(t) &= (1-\mu)\omega E - \gamma I,\\
{}_0^C D_t^{\varphi_1,\cdots,\varphi_r,\varphi_0} A(t) &= \mu\omega' E - \gamma' A,\\
{}_0^C D_t^{\psi_1,\cdots,\psi_r,\psi_0} R(t) &= \gamma I + \gamma' A.
\end{aligned} \tag{55}$$

In this model,

$$\begin{aligned}
{}_0^C D_t^{\xi_1,\cdots,\xi_r,\xi_0} x(t) &= \sum_{i=1}^{r} \lambda_{\xi_i} \cdot {}_0^C D_t^{\xi_i} x(t) + \lambda_{\xi_0} \cdot {}_0^C D_t^{\xi_0} x(t),\\
{}_0^C D_t^{\theta_1,\cdots,\theta_r,\theta_0} x(t) &= \sum_{i=1}^{r} \lambda_{\theta_i} \cdot {}_0^C D_t^{\theta_i} x(t) + \lambda_{\theta_0} \cdot {}_0^C D_t^{\theta_0} x(t),\\
{}_0^C D_t^{\phi_1,\cdots,\phi_r,\phi_0} x(t) &= \sum_{i=1}^{r} \lambda_{\phi_i} \cdot {}_0^C D_t^{\phi_i} x(t) + \lambda_{\phi_0} \cdot {}_0^C D_t^{\phi_0} x(t),\\
{}_0^C D_t^{\varphi_1,\cdots,\varphi_r,\varphi_0} x(t) &= \sum_{i=1}^{r} \lambda_{\varphi_i} \cdot {}_0^C D_t^{\varphi_i} x(t) + \lambda_{\varphi_0} \cdot {}_0^C D_t^{\varphi_0} x(t),\\
{}_0^C D_t^{\psi_1,\cdots,\psi_r,\psi_0} x(t) &= \sum_{i=1}^{r} \lambda_{\psi_i} \cdot {}_0^C D_t^{\psi_i} x(t) + \lambda_{\psi_0} \cdot {}_0^C D_t^{\psi_0} x(t),
\end{aligned}$$

where $0 < \xi_1 < \cdots < \xi_r < \xi_0 = 1, 0 < \theta_1 < \cdots < \theta_r < \theta_0 = 1, 0 < \phi_1 < \cdots < \phi_r < \phi_0 = 1, 0 < \varphi_1 < \cdots < \varphi_r < \varphi_0 = 1, 0 < \psi_1 < \cdots < \psi_r < \psi_0 = 1$, and the weighted coefficients λ_{ξ_i}, λ_{θ_i}, λ_{ϕ_i}, λ_{φ_i} and $\lambda_{\psi_i} \in R^+$ are used to preserve units.

We use the GMMP scheme to discretize this multi-term fractional order nonlinear equation. For the sake of simplicity, we discretize in time using a uniform grid $t_j = jh$, $j = 0, 1, 2, \cdots, n$ and $nh = t$. The multi-term fractional order nonlinear equation can be generally written as:

$${}_0^C D_t^{\alpha_1,\cdots,\alpha_r,\alpha_0} x(t) = f[t_n, x(t_n)], 0 \le t \le T, \tag{56}$$

where $x = (S(t), E(t), I(t), A(t), R(t))^T$ and $0 < \alpha_1 < \cdots < \alpha_r < \alpha_0 = 1$.

Firstly, the Caputo fractional derivative can be discretized as follows:

$${}_0^C D_t^{\alpha_i} x(t_n) = \frac{1}{h^{\alpha_i}} \sum_{k=0}^{n} c_k^{\alpha_i} [x(t_{n-k}) - x(0)], i = 1, 2, \cdots, r, \tag{57}$$

where $c_k^{\alpha_i} = (-1)^k \binom{\alpha_i}{j}$ are binomial coefficients. Hence, we have

$$\begin{aligned}
{}_0^C D_t^{\alpha_1,\cdots,\alpha_r,\alpha_0} x(t_n) &= \sum_{i=1}^{r} \frac{\lambda_i}{h^{\alpha_i}} \sum_{k=0}^{n} c_k^{\alpha_i} [x(t_{n-k}) - x(0)] + \frac{\lambda_0}{h} [x(t_n) - x(t_{n-1})]\\
&= \sum_{k=0}^{n} \sum_{i=1}^{r} \frac{\lambda_i}{h^{\alpha_i}} c_k^{\alpha_i} [x(t_{n-k}) - x(0)] + \frac{\lambda_0}{h} [x(t_n) - x(t_{n-1})]\\
&= \sum_{k=0}^{n} \left[\sum_{i=1}^{r} \frac{\lambda_i}{h^{\alpha_i}} c_k^{\alpha_i} \right] [x(t_{n-k}) - x(0)] + \frac{\lambda_0}{h} [x(t_n) - x(t_{n-1})]\\
&= \sum_{k=0}^{n} B_k^n [x(t_{n-k}) - x(0)] + \frac{\lambda_0}{h} [x(t_n) - x(t_{n-1})],
\end{aligned} \tag{58}$$

where $B_k^n = \sum_{i=1}^{r} \frac{\lambda_i}{h^{\alpha_i}} c_k^{\alpha_i}$.

The discrete scheme of the multi-term fractional order equations (55) is given by

$$ {}_0^C D_t^{\alpha_1,\cdots,\alpha_r,\alpha_0} x(t_n) = f[t_n, x(t_n)], 0 \le t \le T, \tag{59} $$

From the equations (58) and (59), we have

$$ \sum_{k=0}^{n} B_k^n [x(t_{n-k}) - x(0)] + \frac{\lambda_0}{h}[x(t_n) - x(t_{n-1})] = f[t_n, x(t_n)], \tag{60} $$

i.e,

$$ x(t_n) = \frac{f(t_n, x(t_n))}{B_0^n + h^{-1}} + \frac{B_0^n x(0) + \lambda_0 h^{-1} x(t_{n-1})}{B_0^n + \lambda_0 h^{-1}} - \frac{\sum_{k=1}^{n} B_k^n [x(t_{n-k}) - x(0)]}{B_0^n + \lambda_0 h^{-1}}. \tag{61} $$

This implicit difference scheme can also be considered as an equation with respect to an unknown variable $x(t_n)$. The Newton method can be used to solve for the value of $x(t_n)$ of equation (61).

7.2. Application to parameter estimation in the multi-term fractional order SEIAR model of norovirus outbreak

In this section, we consider the following three-term fractional order SEIAR model of the Norovirus outbreak:

$$ \begin{aligned} {}_0^C D_t^{\xi_1,\xi_2,\xi_0} S(t) &= -\beta S(I + \kappa A), \\ {}_0^C D_t^{\theta_1,\theta_2,\theta_0} E(t) &= \beta S(I + \kappa A) - \mu\omega' E - (1-\mu)\omega E, \\ {}_0^C D_t^{\phi_1,\phi_2,\phi_0} I(t) &= (1-\mu)\omega E - \gamma I, \\ {}_0^C D_t^{\varphi_1,\varphi_2,\varphi_0} A(t) &= \mu\omega' E - \gamma' A, \\ {}_0^C D_t^{\psi_1,\psi_2,\psi_0} R(t) &= \gamma I + \gamma' A, \end{aligned} \tag{62} $$

where

$$ \begin{aligned} {}_0^C D_t^{\xi_1,\xi_2,\xi_0} &= \lambda_1 \cdot {}_0^C D_t^{\xi_1} + \lambda_2 \cdot {}_0^C D_t^{\xi_2} + \lambda_3 \cdot {}_0^C D_t^{\xi_0}, \\ {}_0^C D_t^{\theta_1,\theta_2,\theta_0} &= \lambda_4 \cdot {}_0^C D_t^{\theta_1} + \lambda_5 \cdot {}_0^C D_t^{\theta_2} + \lambda_6 \cdot {}_0^C D_t^{\theta_0}, \\ {}_0^C D_t^{\phi_1,\phi_2,\phi_0} &= \lambda_7 \cdot {}_0^C D_t^{\phi_1} + \lambda_8 \cdot {}_0^C D_t^{\phi_2} + \lambda_9 \cdot {}_0^C D_t^{\phi_0}, \\ {}_0^C D_t^{\varphi_1,\varphi_2,\varphi_0} &= \lambda_{10} \cdot {}_0^C D_t^{\varphi_1} + \lambda_{11} \cdot {}_0^C D_t^{\varphi_2} + \lambda_{12} \cdot {}_0^C D_t^{\varphi_0}, \\ {}_0^C D_t^{\psi_1,\psi_2,\psi_0} &= \lambda_{13} \cdot {}_0^C D_t^{\psi_1} + \lambda_{14} \cdot {}_0^C D_t^{\psi_2} + \lambda_{15} \cdot {}_0^C D_t^{\psi_0}, \end{aligned} $$

and the other parameters in this model are defined as the same as those in (36). In order to make the both sides of the equations (62) have the same dimensions about the time t, the parameters $\lambda_i (i = 1, 2, \cdots, 15)$ are introduced on the left sides of the equations. The parameters $\lambda_i (i = 1, 2, 3)$ have dimension of $(days)^{\xi_i - 1} (i = 1, 2, 0)$, and $\lambda_i (i = 4, 5, 6)$ have dimension of $(days)^{\theta_i - 1} (i = 1, 2, 0)$, respectively, The units of the other parameters $\lambda_i (i = 7, 8, \cdots, 15)$ can be obtained similarly. The introduction of these parameters ensures that both sides of the equations have the same dimensions $(days)^{-1}$.

Next, we will use the GMMP scheme to obtain the numerical solution for this three-term fractional order SEIAR model (62), and use the modified hybrid Nelder-Mead simplex search and particle swarm optimization (MH-NMSS-PSO) algorithm to find a suitable set of fractional orders and parameters, with which the three-term fractional SEIAR model (62) can fit the real data. As mentioned above for the one-term fractional order SEIAR model (37), each of the parameters in the three-term SEIAR model (62) has its particular biological meaning and each parameter has a corresponding value range. Therefore, based on these ranges, we select some appropriate intervals and initial velocities as follows:

$$ \begin{aligned} &0 \le \lambda_i = p_i \le 2, i = 1, 2, \cdots, 15, && 0 \le \xi_j = p_{j+15} \le 1, j = 1, 2 \\ &0 \le \theta_k = p_{k+17} \le 1, k = 1, 2, && 0 \le \phi_l = p_{l+19} \le 1, l = 1, 2 \\ &0 \le \varphi_m = p_{m+21} \le 1, m = 1, 2, && 0 \le \psi_n = p_{n+23} \le 1, n = 1, 2 \\ &1 \times 10^{-4} \le \beta = p_{26} \le 1 \times 10^{-3}, && 1 \times 10^{-11} \le \kappa = p_{27} \le 1 \times 10^{-10} \\ &0.01 \le \mu = p_{28} \le 0.3, && 1 \le \omega = p_{29} \le 2, 1 \le \omega' = p_{30} \le 2 \\ &0.3 \le \gamma = p_{31} \le 1, && 0.05 \le \gamma' = p_{32} \le 0.09 \end{aligned} $$

and

$$ V_i = \begin{cases} 0.02 & , \ i = 1, 2, \cdots, 15; \\ 0.01 & , \ i = 16, 17, \cdots, 25; \\ 1 \times 10^{-4} & , \ i = 26; \\ 1 \times 10^{-11} & , \ i = 27; \\ 0.01 & , \ i = 28; \\ 0.025 & , \ i = 29, 30; \\ 0.01 & , \ i = 31, 32. \end{cases} $$

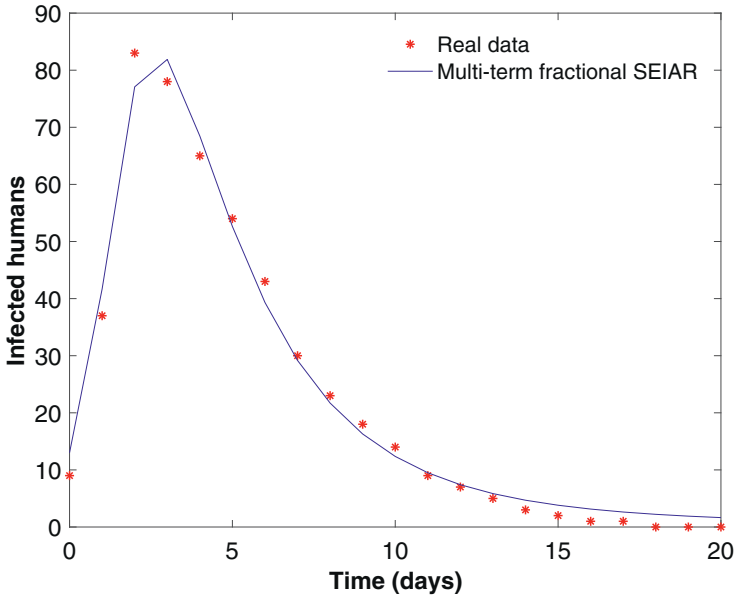

Fig. 2. Number of infected humans $I(t)$ in a middle school in the 2007: Comparison of numerical results of three-term fractional SEIAR model with the real data with the estimated parameters obtained by MH-NMSS-PSO method. The root-mean-square error is rMSE = 2.6041.

Again, using the same initial values and the time as $t = 20$ days, we apply the MH-NMSS-PSO to estimate model parameters from the real data based on the numerical solution solved by the GMMP scheme. Fig. 2 shows the comparison of numerical results of three-term fractional SEIAR model with the real data and the calculated model parameters P^* are:

$$\begin{array}{llll}
\lambda_1 = 0.0049, & \lambda_2 = 1.7476, & \lambda_3 = 0.0450, & \alpha_4 = 2.5174 \times 10^{-4}, \\
\lambda_5 = 0.0017, & \lambda_6 = 1.9998, & \lambda_7 = 0.0038, & \alpha_8 = 7.8341 \times 10^{-4}, \\
\lambda_9 = 0.0377, & \lambda_{10} = 0.4703, & \lambda_{11} = 1.9955, & \lambda_{12} = 0.2186, \\
\lambda_{13} = 0.0095, & \lambda_{14} = 0.1828, & \lambda_{15} = 0.8119, & \xi_1 = 0.6236, \\
\xi_2 = 0.8553, & \theta_1 = 0.6023, & \theta_2 = 0.6000, & \phi_1 = 0.9577, \\
\phi_2 = 0.9495, & \varphi_1 = 0.7814, & \varphi_2 = 0.9898, & \psi_1 = 0.6093, \\
\psi_2 = 0.9324, & \beta = 6.2302 \times 10^{-4}, & \kappa = 1.003 \times 10^{-11}, & \mu = 0.2113, \\
\omega = 1.0018, & \omega' = 1.0012, & \gamma = 0.3026, & \gamma' = 0.0524,
\end{array}$$

As can be seen from Fig. 2 that, the root-mean square error between the numerical solutions of three-term fractional SEIAR model and the real data is rMSE = 2.6041, which implies that the three-term fractional SEIAR model can provide better fit to the real data than the integer order and single-term fractional models.

8. Conclusion

In this paper, we reviewed the fractional epidemic model and proposed a general fractional-order epidemic models system and a multi-term fractional-order SEIAR Model of Norovirus system based on the Caputo fractional derivative. We use the modified hybrid Nelder-Mead simplex search and particle swarm optimization (MH-NMSS-PSO) algorithm to estimate the parameters for fractional differential equations and the multi-term fractional differential equations. Based on the numerical solutions obtained by the GMMP scheme and Newton method, the MH-NMSS-PSO is used to estimate parameters for the single-term and multi-term fractional-order equations. Numerical results show that the GMMP scheme and MH-NMSS-PSO are efficient and valid and the fractional models provide an excellent fit to the real data. Furthermore, the multi-term fractional SEIAR model provides better fit to the real data than the integer order and single-term fractional SEIAR models. This study also demonstrates that the general fraction model mentioned in this paper can predict the number of the infectious people accurately and help the concerned bodies such as policy makers, stake holders and healthy professionals in making well informed decisions in preventing or controlling a potential outbreak in their community, the fractional epidemic models can be a powerful tool that allow us to optimize the use of limited resources of simply to target control measures more efficiently and help us to understand the global dynamics of the spread of infectious disease.

Acknowledgements

This work is supported by the Scholarship of Overseas Studies in the Education Bureau of Fujian Province, the Young and Middle-aged Scholars' Educational Science & Technology Research Project of Fujian Province of China (Grant No. JAT200937),

the National Natural Science Foundation of China (Grant No. 11772046), and the Australian Research Council via the Discovery Projects DP 180103858 and DP 190101889.

References

[1] H.W. Hethcote, The mathematics of infectious diseases, SIAM Rev. 42 (4) (2000) 599–653.
[2] Q. Li, Early transmission dynamics in wuhan, china, of novel coronavirus-infected pnewmonia, The New England Journal of Medicine. 382 (13) (2020) 1199–1207.
[3] P. Martens, How will climate change affect human health? Am. Sci. 87 (1999) 534–541.
[4] H. Heesterbeek, M. Anderson, A.V.B. Sh, D. Angelis, Modeling infectious disease dynamics in the complex landscape of global health, Science (2015) 347.
[5] H.W. Hethcote, L. Gross, T.G. Hallam, S.A. Levin, Springer-verlag, berlin. three basic epidemiological models, Applied Mathematical Ecology (1989) 119–144.
[6] I. Nasell, Stochastic models of some endemic infections, Math. Biosci. 179 (2002) 1–19.
[7] F. Brauer, C. Castillo-Chavez, Mathematical Models in Population Biology and Epidemiology, of Texts, Applied Mathematics, volume 40, Springer, New York, NY, USA, 2001.
[8] W.O. Kermack, A.G. McKendrick, A contribution to mathematical theory of epidemics, Proceedings of the Royal Society A 115 (1927) 700–721.
[9] Q. Yu, D. Reutens, K. O'Brien, V. Vegh, Tissue microstructure features derived from anomalous diffusion measurement in magnetic resonance imaging, Hum. Brain Mapp. 38 (2) (2017) 1068–1081.
[10] S. Qin, F. Liu, I. Turner, V. Vegh, Q. Yu, Q. Yang, Multi-term time fractional bloch equations and application in magnetic resonance imaging, J. Comput. Appl. Math. 319 (2017) 308–319.
[11] Q. Yu, D. Reutens, V. Vegh, Can anomalous diffusion models in magnetic resonance imaging be used to characterise tissue microstructure? Neuroimage 175 (2018) 122–137.
[12] R.M. Anderson, Population dynamics of infectious diseases, Chapman and Hall, London, 1982.
[13] R.M. Anderson, R.M. May, Population biology of infectious diseases, Springer-Verlag, Berlin, Heidelberg, New York, 1982.
[14] T. Sardar, S. Rana, S. Bhattacharya, K. Al-Khaled, J. Chattopadhyay, A generic model for a single strain mosquito-transmitted disease with memory on the host and the vector, Math. Biosci. 263 (2015) 18–36.
[15] J. Rosenbaum, M.B. Nathan, R. Ragoonanansingh, S. Rawlins, C. Gayle, et al., Community participation in dengue prevention and control: a survey of knowledge, attitudes, and practice in trinidad and tobago, Amer. J. Trop. Med. Hygiene 53 (2) (1995) 111–117.
[16] A. Acharya, K. Goswami, S. Srinath, A. Goswami, Awareness about dengue syndrome and related preventive practices amongst residents of an urban resettlement colony of south delhi, J. Vect. Borne. Dis. 42 (2005) 122–127.
[17] K.B. Oldham, J. Spanier, The fractional calculus, Academic Press, New York, 1974.
[18] D. Baleanu, K. Diethelm, E. Scalas, J.J. Trujillo, Fractional calculus: Models and numerical methods, World Scientific Publishing, Singapore, 2012.
[19] K. Diethelm, The analysis of fractional differential equations, Springer, Berlin, vol. 9, 2004, pp. 1333–1341.
[20] X. Jiang, H. Qi, Thermal wave model of bioheat transfer with modified riemann-liouville fractional derivative, J. Phys. A Math. Theor. 45 (2012) 4851011–48510111.
[21] M.R.L. Fractional, Calculus in bioengineering, Connecticut: Begel House Publishers, Inc., 2006.
[22] R. Magin, Fractional calculus models of complex dynamics in biological tissues, Comput. Math. Appl. 59 (2010) 1586–1593.
[23] F.L. Burrage, N.A. Hamilton, Some novel techniques of parameter estimation for dynamical models in biological systems, IMA J. Appl. Math. 78 (2013) 235–260.
[24] O.O. Mizrak, C. Mizrak, A. Kashkynbayev, Y. Kuang, Can fractional differentiation improve stability results and data fitting ability of a prostate cancer model under intermittent androgen suppression therapy? Chaos, Solitons and Fractals 131 (2020) 09529.
[25] S. Qin, F. Liu, I. Turner, Q. Yu, Q. Yang, V. Vegh, Characterization of anomalous relaxation using the time-fractional bloch equation and multiple echo t2*-weighted magnetic resonance imaging at 7t, Magn. Reson. Med. 77 (2017) 1485–1494.
[26] F. Liu, V. Anh, I. Turner, Numerical solution for the space fractional fokker-planck equation, J. Comput. Appl. Math. 166 (2004) 209–219.
[27] I. Podlubny, Fractional differential equations, Academic Press, New York, 1999.
[28] A.A. Kilbas, H.M. Srivastava, J.J. Trujillo, Theory and applications of fractional differential equations, North-Holland Mathematics Studies, Elsevier Science B.V., Amsterdam, vol. 204, 2006.
[29] I. Petras, Fractional-Order nonlinear systems: Modeling, analysis and simulation, Higher Education Press, Beijing, 2011.
[30] Y. Ding, Z. Wang, H. Ye, Optimal control of a fractional-order HIV-immune system with memory, IEEE Trans. Control Syst. Technol. 99 (2011) 1–7.
[31] M. El-Shahed, A. Alsaedi, The fractional SIAC model and influenza a, Math. Probl. Eng. (2011) 4803781–4803789.
[32] E. Hanert, E. Schumacher, Front dynamics in fractional-order epidemic modes, J. Theor. Biol. 279 (2011) 9–16.
[33] H.S. Rodrigues, M.T.T. Monteiro, D.F.M. Torres, Math. Comput. Modelling 52 (2010) 1667–1673.
[34] H.S. Rodrigues, M.T.T. Monteiro, D.F.M. Torres, In numerical analysis and applied mathematics, T. Simos, AIP Conf. Proc. 1281 (2010) 979–982.
[35] H.S. Rodrigues, M.T.T. Monteiro, D.F.M. Torres, A. Zinober, Int. J. Comput. Math. (2011).
[36] S.P. Ansari, S.K. Agrawal, And subir das, stability analysis of fractional order generalized chaotic SIR epidemic model and its synchronization using active control method, journal of physics 84 (2014) 23–32.
[37] S. Samko, A. Kilbas, O. Marichev, Fractional integrals and derivatives: theory and applications, Gordon and Breach, Amsterdam (1993).
[38] V. Lakshmikantham, A. Vatsala, Basic theory of fractional differential equations, Nonlinear Analysis: Theory, Methods and Applications 69 (8) (2008) 2677–2682.
[39] R. Agarwal, M. Benchohra, S. Hamani, A survey on existence results for boundary value problems of nonlinear fractional differential equations and inclusions, Acta Appl. Math. 109 (2010) 973–1033.
[40] J.C. Semenza, B. Menne, The Lancet Infectious Diseases 9 (2009) 365–375.
[41] WHO, T. dengue: Guidelines for diagnosis, treatment, prevention and control. geneva, WHO Library, 2009, pp. 10–12.
[42] H. Nishiura, Mathematical and statistical analyses of the spread of dengue, Dengue Bull 30 (2006) 51–67.
[43] S. Hales, N. De Wet, J. Maindonald, A. Woodward, Potential effect of population and climate changes on global distribution of dengue fever: an empirical model, Lancet 360 (2002) 830–834.
[44] H. Rodrigues, M. Monteiro, D. Torres, A. Zinober, Dengue disease, basic reproduction number and control, Int. J. Comput. Math. 89 (2012) 334–346.
[45] T. Sardar, S. Rana, J. Chattopadhyay, A mathematical model of dengue transmission with memory, Commun. Nonlinear Sci. Numer. Simul. 22 (2015) 511–552.
[46] S. Pooseh, H. Rodrigues, S. Torres, Fractional derivatives in dengue epidemics, Numer. Anal. Appl. Math. ICNAAM (2011) 739–742.
[47] K. Diethelm, A fractional calcus based model for the simulation of an outbreak of dengue fever, Nonlin. Dy. 71 (2013) 613–619.
[48] T. Li, Y. Wang, F. Liu, I. Turner, Novel parameter estimation techniques for a multi-term fractional dynamical epidemic model of dengue fever, Numer. Algorithms (2019).
[49] N. Hamdan, A. Kilicman, Analysis of the fractional order dengue transmission model: a case study in malaysia, Advances in Difference Equations (2019) 1–13.
[50] H. Al-Sulami, M. El-Shahed, J.J. Nieto, W. Shammakh, On fractional order dengue epidemic model, Hindawi Publishing Corporation Mathematical Problems in Engineering 2014 (2014) 6. Article ID 456537
[51] A.K. Nur'Izzati, A fractional order SIR epidemic model for dengue transmission, Chaos, Solitons and Fractals 114 (2018) 55–62.

[52] O. Defterli, Modeling the impact of temperature on fractional order dengue model with vertical transmission, An International Journal of Optimization and Control: Theories and Applications 10 (1) (2020) 85–93. ISSN:2146-0957, eISSN:2146-5703
[53] G. Zaman, Dynamical behavior of leptospirosis disease and role of optimal control theory, Int. J. Comput. Math. 7 (2010). Article J10
[54] G. Zaman, M. Altaf Khan, S. Islam, M.I. Chohan, I.H. Jung, Modeling dynamical interactions between leptospirosis infected vector and human population, Applied Mathematical Sciences 6 (25–28) (2012) 1287–1302.
[55] M.A. Khan, G. Zaman, S. Islam, M.I. Chouhan, Optimal campaign in leptospirosis epidemic by multiple control variables, Appl. Math. (Irvine) 3 (11) (2012) 1655–1663.
[56] M.A. Khan, S. Islam, S.A. Khan, G. Zaman, Global stability of vector-host disease with variable population size, Biomed. Res. Int. 2013 (2013) 9. Article ID 710917
[57] M.A. Khan, S. Islam, S.A. Khan, Mathematical modeling towards the dynamical interaction of leptospirosis, Applied Mathematics and Information Sciences 8 (3) (2014) 1049–1056.
[58] S.F. Saddiq, M.A. Khan, S. Islam, G. Zaman, N. Khalid, S.I.A. Shah, Optimal control of an epidemic model of leptospirosis with time delay, Life Sci. J. 10 (3) (2013) 292–298.
[59] M.A. Khan, S.F. Saddiq, S. Islam, I. Khan, D.L.C. Ching, Epidemic model of leptospirosis containing fractional order, Abstract and Applied Analysis 2014 (2014) 8. Article ID 317201
[60] R. Casagrandi, L. Bolzoni, S.A. Levin, V. Andreasen, The SIRC model and influenza a, Math. Biosci. 200 (2) (2006) 152–169.
[61] M. El-Shahed, A. Alsaedi, The fractional SIRC model and influenza a, Mathematical Problems in Engineering (2011) 9. Article ID 480378
[62] F.A. Rihan, D. Baleanu, S. Lakshmanan, R. Rakkiyappan, On fractional SIRC model with salmonella bacterial infection, Abstract and Applied Analysis 2014 (2014) 9. Article ID 136263
[63] L. Jódar, R.J. Villanueva, A.J. Arenas, G.C. González, Nonstandard numerical methods for a mathematical model for influenza disease, Math. Comput. Simul. 79 (3) (2008) 622–633.
[64] CDC, H1n1 flu. center for disease control and prevention website. Available from: http://www.cdc.gov/h1n1flu/.
[65] S. Takeuchi, Y. Kuroda, Predicting spread of new pandemic swine-origin influenza a (h1n1) in local mid-size city: evaluation of hospital bed shortage and effectiveness of vaccination, Nippon Eiseigaku Zasshi 65 (1) (2010) 48–52.
[66] G.F. Webb, Y.H. Hsieh, J. Wu, M.J. Blaser, Pre-symptomatic influenza transmission, surveillance, and school closings: implications for novel influenza a (h1n1), Math. Model Nat. Phenom. 5 (3) (2010) 191–205.
[67] S. Tracht, S. Del Valle, J. Hyman, Mathematical modeling of the effectiveness of facemasks in reducing the spread of novel influenza a (h1n1), PLoS ONE 5 (2) (2010). E9018
[68] S. Towers, Z. Feng, Pandemic h1n1 influenza: predicting the course of a pandemic and assessing the efficacy of the planned vaccination programme in the united states, Euro Surveill 14 (41) (2009) 1–3.
[69] J. Ong, M. Chen, A. Cook, H. Lee, V. Lee, R. Lin, P. Tambyah, L. Goh, Real-time epidemic monitoring and forecasting of h1n1-2009 using influenza-like illness from general practice and family doctor clinics in singapore, PLoS ONE 5 (4) (2010). E10036
[70] H. Hethcote, Mathematics of infectious diseases, SIAM Rev. 42 (4) (2005) 599–653.
[71] J.D. Murray, Mathematical Biology I, An Introduction, Springer: Berlin, 2002.
[72] S. Whang, S. Choi, E. Jung, A dynamic model for tuberculosis transmission and optimal treatment strategies in south korea, J. Theor. Biol. 279 (1) (2011) 120–131.
[73] J. Zhang, Z. Jin, G.Q. Sun, T. Zhou, S. Ruan, Analysis of rabies in china: transmission dynamics and control, PLoS ONE 6 (7) (2011). E20891
[74] G.G. Parra, A.J. Arenas, B.M.C. Charpentier, A fractional order epidemic model for the simulation of outbreaks of influenza a(h1n1), Math. Methods Appl. Sci. 37 (2014) 2218–2226.
[75] Centers for disease control and prevention, Epidemiology of measles–United States, 1998, MMWR 48 (1999) 749–753.
[76] M.S. Bartlett, Measles periodicity and community size, Journal of the Royal Statistical Society A (120) (1957) 48–70.
[77] E.F.D. Goufo, S.C.O. Noutchie, S. Mugisha, A fractional SEIR epidemic model for spatial and temporal spread of measles in metapopulations, Abstract and Applied Analysis 2014 (2014) 6. Article ID 781028
[78] J. Arino, P. van den Driessche, Metapopulation epidemic models. a survey, Fields Institute Communications 48 (2006) 1–13.
[79] L.A. Rvachev, I.M. Longini Jr., A mathematical model for the global spread of influenza, Math. Biosci. 75 (1) (1985) 3–22.
[80] F.A. Abdullah, F. Liu, P. Burrage, K. Burrage, T. Li, Novel analytical and numerical techniques for fractional temporal SEIR measles model, Numer. Algorithms 79 (1) (2017) 19–40.
[81] R. Gorenflo, F. Mainardi, D. Moretti, P. Paradisi, Time fractional diffusion: a discrete random walk approach, Nonlinear Dyn. 29 (2002) 129–143.
[82] J. Arino, C.C. McCluskey, P. van den Driessche, Global results for an epidemic model with vaccination that exhibits backward bifurcation, SIAM J. Appl. Math. 64 (1) (2003) 260–276.
[83] S. Gandon, M. Mackinnon, S. Nee, A. Read, Imperfect vaccination: some epidemiological and evolutionary consequences, Proc. Roy. Soc. Lond., Series B 270 (2003) 1129–1136.
[84] A.B. Gumel, C.C. McCluskey, J. Watmough, AN SVEIR MODEL FOR ASSESSING POTENTIAL IMPACT OF AN IMPERFECT ANTI-SARS VACCINE, MATHEMATICAL BIOSCIENCES AND ENGINEERING 3 (3) (2006).
[85] H. Wei, Y. Jiang, X. Song, G.H. Su, S.Z. Qiu, Global attractivity and permanence of a SVEIR epidemic model with pulse vaccination and time delay, J. Comput. Appl. Math. 229 (2009) 302–312.
[86] M.E. Hajji, S. Sayari, Analysis of a fractional-order SVEIR epidemic model with a general nonlinear saturated incidence rate in a continuous reactor, Asian Research Journal of Mathematics 12 (4) (2019) 1–17.
[87] J.A. Levy, Pathogenesis of human immunodeficiency virus infection, Microbiol. Rev. 57 (1993) 183–289.
[88] C. Stoddart, R. Reyes, Models of HIV-1 disease: a review of current status, drug discovery today, Disease 3 (1) (2006) 113–119.
[89] R.M. Anderson, The role of mathematical models in the study of HIV transmission and the epidemiology of AIDS, J. AIDS 1 (1988) 241–256.
[90] R.M. Anderson, G.F. Medly, R.M. May, A.M. Johnson, A preliminary study of the transmission dynamics of the human immunodeficiency virus (HIV), the causative agent of AIDS, IMA J. Math. Appl. Med. Biol 3 (1986) 229–263.
[91] R.M. May, R.M. Anderson, Transmission dynamics of HIV infection, Nature 326 (1987) 137–142.
[92] M. Bachar, A. Dorfmayr, HIV Treatment models with time delay, C. R. Biologies 327 (2004) 983–994.
[93] S. Blower, Calculating the consequences: HAART and risky sex, AIDS 15 (2001) 1309–1310.
[94] C. Connell, Mccluskey, a model of HIV/AIDS with staged progression and amelioration, Math. Biosci 181 (2003) 1–16.
[95] H.W. Hethcote, J.W.V. Ark, Modelling HIV Transmission and AIDS in the United States, Lect. Notes Biomath, vol. 95, Springer, Berlin, 1992.
[96] C. Castillo-Chavez, Mathematical and statistical approaches to AIDS epidemiology, lecture notes in biomath. 83, Springer-Verlag, Berlin, 1989.
[97] M. Javidi, N. Nyamoradi, Numerical behavior of a fractional order HIV/AIDS epidemic model, World Journal of Modelling and Simulation 9 (2) (2013) 139–149.
[98] H. Kheiri, M. Jafari, Fractional optimal control of an HIV/AIDS epidemic model with random testing and contact tracing, J. Appl. Math. Comput. 60 (2019) 387–411.
[99] A. Mastroberardino, Y. Cheng, A. Abdelrazec, H. Liu, Mathematical modeling of the HIV/AIDS epidemic in cuba, Int. J. Biomath 08 (2015) 1550047, doi:10.1142/S1793524515500473.
[100] C. Gorry, Cubas HIV/AIDS strategy: An integrated, rights-Based approach, Oxfam International, Havana, 2008.
[101] V.S. Erturk, G. Zaman, S. Momani, A numeric analytic method for approximating a giving up smoking model containing fractional derivatives, Comput. Math. Appl. 64 (2012) 3068–3074.
[102] G. Zaman, Optimal campaign in the smoking dynamics, Comput. Math. Methods Med (2011). Article ID 163834

[103] G. Zaman, Qualitative behavior of giving up smoking models, Bull. Malays. Math. Soc. 34 (2011) 403–415.
[104] J.L. Lubin, Z.E. Caporaso, Cigarette smoking and lung cancer: modeling total exposure and intensity, Cancer Epidemiol. Biomark. Prev. 15 (2006) 517–523.
[105] C.C. Garsow, G.J. Salivia, A.R. Herrera, Mathematical models for the dynamics of tobacoo use, recovery and relapse, Technical Report Series BU-1505-M, Cornell University, UK, 2000.
[106] O. Sharomi, A.B. Gumel, Curtailing smoking dynamics: a mathematical modeling approach, Appl. Math. Comput. 195 (2008) 475–499.
[107] A. Zeb, I. Chohan, G. Zaman, The homotopy analysis method for approximating of giving up smoking model in fractional order, Appl. Math. 3 (2012) 914–919.
[108] Z. Alkhudhari, S. Al-Sheikh, S. Al-Tuwairqi, Global dynamics of a mathematical model on smoking, Appl. Math. (2014). Article ID 847075
[109] M. Khalid, F.S. Khan, A. Iqbal, Perturbation-iteration algorithm to solve fractional giving up smoking mathematical model, Int. J. Comput. Appl. 142 (2016) 1–6.
[110] M. Abdullah, A. Ahmad, N. Raza, M. Farman, M.O. Ahmad, Approximate solution and analysis of smoking epidemic model with caputo fractional derivatives, Int. J. Appl. Comput. Math. 4 (2018) 112.
[111] P. Veeresha, D. G. Prakasha, H.M. Baskonus, Solving smoking epidemic model of fractional order using a modifed homotopy analysis transform method, Mathematical Sciences (2019). Accepted: 10 April
[112] K.L. Kotloff, J.P. Winickoff, B. Ivanoff, J.D. Clemens, D.L. Swerdlow, et al., Global burden of shigella infections: implications for vaccine development and implementation of control strategies, Bull. World Health Organ 77 (1999) 651–666.
[113] C.S. Chiou, W.B. Hsu, H.L. Wei, J.H. Chen, Molecular epidemiology of a shigella flexneri outbreak in a mountainous township in taiwan, republic of china, J. Clin. Microbiol. 39 (2001) 1048–1056.
[114] D.L. Martin, T.L. Gustafson, J.W. Pelosi, L. Suarez, G.V. Pierce, Contaminated produce, a common source for two outbreaks of shigella gastroenteritis, Am. J. Epidemiol. 124 (1986) 299–305.
[115] G. Samonis, L. Elting, E. Skoulika, S. Maraki, Y. Tselentis, An outbreak of diarrhoeal disease attributed to shigella sonnei, Epidemiol. Infect. 112 (1994) 235–245.
[116] W. Swaddiwudhipong, S. Karintraratana, S. Kavinum, A common-source outbreak of shigellosis involving a piped public water supply in northern thai communities, J. Trop. Med. Hyg. 98 (1995) 145–150.
[117] F. He, K. Han, L. Liu, W. Sun, L. Zhang, et al., Shigellosis outbreak associated with contaminated well water in a rural elementary school: sichuan province, china, june 7–16, 2009, PLoS ONE 7 (2012). E47239
[118] P.S. Mead, L. Slutsker, V. Dietz, L.F. McCaig, J.S. Bresee, et al., Food-related illness and death in the united states, Emerg. Infect. Dis. 5 (1999) 607–625.
[119] H.L. Dupont, Shigella species (bacillary dysentery), Principles and practices of infectious diseases. 5th ed. Philadelphia: Churchill Livingstone, 2000, pp. 2363–2368.
[120] J.T. Wu, B.J. Cowling, The use of mathematical models to inform influenza pandemic preparedness and response, Exp. Biol. Med. (Maywood) 236 (2011) 955–961.
[121] I.M. Longini Jr., A. Nizam, S. Xu, K. Ungchusak, W. Hanshaoworakul, et al., Containing pandemic influenza at the source, Science 309 (2005) 1083–1087.
[122] Y. Yang, J.D. Sugimoto, M.E. Halloran, N.E. Basta, D.L. Chao, et al., The transmissibility and control of pandemic influenza a (h1n1) virus, Science 326 (2009) 729–733.
[123] S. Tang, Y. Xiao, Y. Yang, Y. Zhou, J. Wu, et al., Community-based measures for mitigating the 2009 h1n1 pandemic in china, PLoS ONE 5 (2010). E10911
[124] M.Z. Gojovic, B. Sander, D. Fisman, M.D. Krahn, C.T. Bauch, Modelling mitigation strategies for pandemic (h1n1), CMAJ 181 (2009) 673–680.
[125] Z.G. Bai, Y.C. Zhou, Threshold dynamics of a bacillary dysentery model with seasonal fluctuation, Discrete Continuous Dyn. Syst. Ser.-B 15 (2011) 1–14.
[126] J.H. Tien, D.J.D. Earn, Multiple transmission pathways and disease dynamics in a waterborne pathogen model, Bull. Math. Biol. 72 (2010) 1506–1533.
[127] T. Chen, R.K.-k. Leung, Z. Zhou, R. Liu, X. Zhang, L. Zhang, Investigation of key interventions for shigellosis outbreak control in china, PLoS ONE 9 (4) (2014), doi:10.1371/journal.pone.0095006. E95006
[128] M. de Wit, M. Koopmans, L. Kortbeek, et al., A population-based cohort study on gastroenteritis in the netherlands: incidenceand etiology, Am. J. Epidemiol. 154 (7) (2001) 666–674.
[129] E. Scallan, R. Hoekstra, F. Angulo, et al., Foodborneillness acquired in the united states major pathogens, Emerg Infect Dis 17 (1) (2011) 7–15.
[130] M. Patel, M. Widdowson, R. Glass, et al., Systematicliterature review of role of noroviruses in sporadic gastroenteritis, EmergInfect Dis 14 (8) (2008) 1224–1231.
[131] B. Lopman, A. Hall, A. Curns, et al., Increasingrates of gastroenteritis hospital discharges in US adults and the contributionof norovirus, 1996–2007, Clin. Infect. Dis. 52 (4) (2011) 466–474.
[132] A. Hall, A. Curns, L. McDonald, et al., The roles ofclostridium difficile and norovirus among gastroenteritis-associated deaths in the united states 1999–2007, Clin. Infect. Dis. 55 (2) (2012) 216–223.
[133] B. Lopman, G. Adak, M. Reacher, et al., Twoepidemiologic patterns of norovirus outbreaks: surveillance in england andwales 1992–2000, Emerg. Infect. Dis. 9 (1) (2003) 71–77.
[134] P. Teunis, C. Moe, P. Liu, et al., Norwalk virus: how infectious is it? J. Med. Virol. 80 (8) (2008) 1468–1476.
[135] Is there a population awareness of microbes: the dynamics of norovirus transmission, CTModelling (2018). Available at https://mp.weixin.qq.com/s/gMdemZE1Vl1r4DHuDqPoQw
[136] F. Liu, K. Burrage, Novel techniques in parameter estimation for fractional dynamical models arising from biological systems, Comput. Math. Appl. 62 (3) (2011) 822–833.
[137] T. Li, Y. Wang, M. Luo, Control of chaotic and hyperchaotic systems based on a fractional order controller, Chin. Phys. B 23 (2014) 0805011–08050111.
[138] S. Yuste, J. Murillo, On three explicit difference schemes for fractional diffusion and diffusion-wave equations, Physica Scripta, T 136 (2009) 14–25.
[139] J.A. Nelder, R. Mead, A simplex method for function minimization, Comput. J. 7 (1965) 308–313.
[140] R.C. Eberhart, J. Kennedy, A New Optimizer Using Particle Swarm Theory, in: in Proceedings of the sixth international symposium on micro machine and human science, vol. 1, New York, NY, 1995, pp. 39–43.
[141] J. Robinson, Y. Rahmat-Samii, Particle swarm optimization in electromagnetics, IEEE Trans. Antennas Propag. 52 (2) (2004) 397–407.